

**MECHANISM OF TRIBOELECTRICITY: A
NOVEL PERSPECTIVE FOR STUDYING
CONTACT ELECTRIFICATION BASED ON
METAL-POLYMER AND
POLYMER-POLYMER INTERACTIONS**

A THESIS SUBMITTED TO
THE GRADUATE SCHOOL OF ENGINEERING AND SCIENCE
OF BILKENT UNIVERSITY
IN PARTIAL FULFILLMENT OF THE REQUIREMENTS FOR
THE DEGREE OF
MASTER OF SCIENCE
IN
MATERIALS SCIENCE AND NANOTECHNOLOGY

By
Umar Gishiwa Musa
August 2016

MECHANISM OF TRIBOELECTRICITY: A NOVEL PERSPECTIVE FOR STUDYING CONTACT ELECTRIFICATION BASED ON METAL-POLYMER AND POLYMER-POLYMER INTERACTIONS

By Umar Gishiwa Musa

August 2016

We certify that we have read this thesis and that in our opinion it is fully adequate, in scope and in quality, as a thesis for the degree of Master of Science.

Hasan Tarik Baytekin(Advisor)

Eda Yılmaz

Akin Akdağ

Approved for the Graduate School of Engineering and Science:

Levent Onural
Director of the Graduate School

ABSTRACT

MECHANISM OF TRIBOELECTRICITY: A NOVEL PERSPECTIVE FOR STUDYING CONTACT ELECTRIFICATION BASED ON METAL-POLYMER AND POLYMER-POLYMER INTERACTIONS

Umar Gishiwa Musa

M.S. in Materials Science And Nanotechnology

Advisor: Hasan Tarik Baytekin

August 2016

The static electricity that is generated when two identical or different materials come in contact with each other and separated is a well known physical phenomenon that has been studied for over 25 centuries. Contact charging occurs in technological and natural aspects of our everyday life. Generation of lightning and the feeling of unexpected shocks on dry days are excellent examples of naturally occurring phenomenon, while in technology it is used for photocopying and laser printing. Owing to the increase in energy consumption around the globe and demand for carbon emissions free energy sources, the triboelectric effect has recently being utilized as an effective means of harvesting mechanical energy and converting it into electricity for novel applications like powering portable electronic devices and self powered active sensing. Despite the fact that it has been known and applied for many years, the fundamental mechanism of contact electrification is still not fully understood.

This study proposes a mechanism for triggering such triboelectric charge based on polymer-polymer and metal-polymer interactions. Conventionally, the mechanism of electrostatic charge generation is being presumed as a process giving rise to a combination of positive (arising from contact) and negative (arising from separation) charges in every single contact and separation. However, in our mechanism we propose a concept that shows combination of both positive and negative charges as “contact” and either positive or negative charge, depending on the initial contact-charge polarity of the material (due to surface charge mosaic), as “separation” charge. Different kinds of polymers like polydimethylsiloxane (PDMS), polytetrafluoroethylene (PTFE), Polyethersulfone (PES) and polypropene (PP) were used in this study and similar characteristic was observed

for all of the polymers. Thus, our perception of the working principle of triboelectrification between two dielectric materials or a metal and a dielectric material is consistent and potentially vital in comprehending some unresolved controversies on triboelectricity.

Keywords: Contact electrification, Mechanism, Triboelectricity, Polymer, Triboelectric charge, Contact and Separation.

ÖZET

TRİBOELEKTRİĞİN MEKANİZMASI: METAL-POLİMER VE POLİMER-POLİMER ETKİLEŞİMİ TABANLI KONTAKT ELEKTRİKLENMEDE YENİ BİR KONSEPT

Umar Gishiwa Musa

Malzeme Bilimi ve Nanoteknoloji, Yüksek Lisans

Tez Danışmanı: Hasan Tarik Baytekin

Ağustos 2016

İki aynı veya farklı tür maddeden oluşan yüzeyin birbirine dokundurulup uzaklaştırılması sonucu oluşan statik elektrik, 25 yüzyıldan beri çalışılmakta olup çok iyi bilinen fiziksel bir olgudur. Kontakt yüklenme günlük yaşamımızda bir çok doğal ve teknolojik varlıkta meydana gelmektedir. Kontakt elektrikleme fotokopi ve yazıcı teknolojisinde kullanılır, gökyüzünde şimşek oluşumu ve cisimler arasında meydana gelen beklenmedik elektrik şokları ise kontakt elektriklemenin doğadaki mükemmel örnekleridir. Dünyada enerji tüketiminin ve karbon emisyonu yok olan kaynaklara ihtiyacın artmasından dolayı son yıllarda triboelektrik, taşınabilir cihazların şarj edilmesi ve kendi kendini şarj eden sensörler gibi yeni uygulamalar için mekanik enerjiyi elektrik enerjisine dönüştürmede etkili bir yol olarak kullanılmaktadır. Yıllardır biliniyor ve kullanılıyor olmasına rağmen, kontakt elektriklemenin mekanizması halen tam olarak açıklığa kavuşmamıştır.

Bu çalışmada metal-polimer ve polimer-polimer etkileşimi tabanlı yeni bir triboelektrik tetikleme mekanizması sunulmaktadır. Geleneksel olarak elektrostatik yük oluşumu, pozitif yükün kontakt sırasında oluşması ve negatif yükün ise ayrılma sırasında oluşması proseslerinin bir kombinasyonu olarak kabul edilmektedir. Bu tezde sunulan mekanizmada ise, pozitif ve negatif yük oluşumları kombinasyonunun yüzeylerin kontakt sırasındaki yük polaritesine (mozaik yüzey yük modeli) bağlı olarak hem kontakt hem de ayrılmada görülebileceğini göstermekteyiz. Bu çalışmada, polidimetilsiloksan (PDMS), politetrafloroetilen (PTFE), polietersülfon (PES) ve polipropilen (PP) gibi farklı tür polimerler kullanıldı ve her bir polimer için benzer özellikler gözlenmiştir. Çalışmamızda, iki

dielektrik ya da bir dielektrik ve bir metal arasındaki triboelektriklenme mekanizması için sunduğumuz yeni bakışın geçerliliği gösterilmiştir ve bu bakış, triboelektriklenme konseptinde var olan tartışmanın açıklığa kavuşmasında büyük öneme sahiptir.

Anahtar sözcükler: Kontakt elektrikleme, Mekanizma, Triboelektrik, Polimer, Triboelektrik Yük, Temas ve Ayrılma..

Acknowledgement

I would like to express my gratitude to my advisor, Asst. Prof. Dr. H. Tarik Baytekin for his enthusiastic support and guidance throughout my thesis. He has given me all the essential advice and inspiration throughout my course of study. I believe his passionate research techniques will have numerous contributions to my scientific prospects. I would also like to thank my co-advisor, Prof. Mehmet Bayindir for his effort and support in this scientific journey.

My special thanks to Dr. Mehmet Kanik for his advice, motivation and confidence in me during this expedition. I am grateful to Mrs. NeŞe Özgür for her fervent support throughout this journey. I would love to express my sincere appreciation to Muhammad Yunusa and Pınar Beyaz kılıç for their assistance throughout this journey. I would like to thank the rest of my office mates, former and present research colleagues; Mustafa Ürel, Ahmet Faruk Yavuz, Mehmet Giray Say, Zelal Yavuz, and Doruk Cezan for having good times together and being helpful to one another.

I would like to express my sincere gratitude to some of my friends who are like brothers to me and have tirelessly helped me not only academically, but also intellectually. In particular Abba Usman Saleh, Abubakar Isa Adamu, Shettima Sani Dambatta, Abdullahi adamu, Oyewole Benjamin Efunbajo, Adamu Abdullahi, and Musa Abdullahi. I would like to thank the entire National Nanotechnology Research Center (UNAM) family for their support.

Last but not the least, words are powerless to express my gratitude to my beloved family, especially my parents who have had sleepless nights to see my success every now and then. I am so grateful to them, including my brothers and sisters for their prayers and support in my everyday activities.

Thanks to Scientific and Technological Research Council of Turkey (TÜBİTAK), who supported this work under project no: 214M358.

Contents

1	Motivation	1
2	Introduction	3
2.1	Triboelectricity	3
2.1.1	History of triboelectricity	5
2.1.2	Triboelectric effect	6
2.1.3	Consequences of tribo-effect	7
2.2	Theory of the Charge transfer mechanisms	10
2.2.1	Electron transfer	12
2.2.2	Ion transfer	15
2.2.3	Material transfer	15
2.3	Triboelectric series	16
3	Contact electrification and tribocharge generation for metal-polymer and polymer-polymer interactions	18

CONTENTS ix

3.1 Introduction 18

3.2 Experimental Section 22

 3.2.1 Polymer film preparation 22

 3.2.2 Voltage and current measurement 22

 3.2.3 Surface characterization 25

3.3 Results and discussions 25

3.4 Mechanism of contact electrification 37

 3.4.1 Mechanism of metal-polymer tribocharging 38

 3.4.2 Mechanism of polymer-polymer tribocharging 48

4 Conclusion 51

Bibliography 52

A Arduino codes 63

B Device control system 65

C Circuit diagram 66

D Data processing 67

List of Figures

2.1	Naturally occurring and technologically applied triboelectric phenomena	4
2.2	Energy harvesting from water-flow and human-mouth wind	9
2.3	Other examples of energy harvesting devices	10
2.4	Surface charge transfer between metal-metal contact.	12
2.5	Surface states of metal-polymer, before and after contact.	13
2.6	Surface states of polymer-polymer, before and after contact.	14
2.7	Triboelectric series of some materials	17
3.1	Unexplained literature results showing our proposed mechanism	20
3.2	More literature results practically showing our proposed mechanism	21
3.3	Mechanical tapping device for electrical characterization of polymers using contact electrification.	24
3.4	Measurement setup for the experiment: (a) Output voltage measurement. (b) Short circuit current measurement.	24

3.5	Contact and separation signals obtained from interaction between 12 mm diameter aluminium metal and two different 18 mm diameter polymers (PDMS and PTFE) at low, moderate, and high frequencies	27
3.6	More results of interaction between 12 mm diameter aluminium metal and eight different 18 mm diameter polymers at low frequency for verification of our proposed contact electrification mechanism	29
3.7	Signals showing positive charge from interaction of metal with (a) PC and (b) Nylon at low frequency.	29
3.8	Detailed information of the contact and separation between PDMS and aluminium metal, clearly showing CE, SE, convergence and divergence induction (I_c and I_d) on both materials during and after contact. (a) Overall signal (b) Signal from base electrode (c) Signal from metal electrode.	30
3.9	XPS surface analysis of PDMS and Al after contact and separation, for investigation of material transfer and separation energy	32
3.10	Short circuit current and open circuit voltage obtained from thickness test of PDMS in contact with Cu metal at 1.0 and 10.0 Hz, respectively. Results from contact between Cu metal and PDMS of thickness: (a) 0.15 mm, (b) 0.24 mm, (c) 0.41 mm, and (d) 0.55 mm.	35
3.11	Open-circuit voltage, short circuit current and power density dependence on thickness, and output power versus relative humidity relations	37
3.12	Proposed mechanism of contact electrification based on metal-polymer interaction at low and moderate frequency	40

3.13	Behaviour of the signals after first contact and separation based on metal-polymer interaction at low and moderate frequency contacts, where not only separation (SE) and contact (CE) electrification signals are obtained but also charge induction signals appear while the materials are converging and diverging	42
3.14	Overall outcome of metal-polymer contacts with their respective channel signals	43
3.15	Design of contact base electrode with polymer diameter 12 mm and metal electrode of metal electrode of 6 mm diameter. (b) Picture showing BE with polymer thin film and ME	45
3.16	Electron transfer from polymer to metal contact electrification with LED connected	47
3.17	(a) Samples used. From left to right; (i) Pure PDMS, AuNp-PDMS composites (ii) 0.5, (iii) 0.99, (iv) 1.96 and (v) 3.85 % of Au in 1 gram of PDMS each. (b) SEM images of pure PDMS at magnification of 564 x, and (c) Au doped PDMS (5 mg Au in 1 gram of PDMS = 1.96 %) with 539 x magnification and the percentages of gold in 1 gram of PDMS.	49
3.18	Signals obtained by doping pure PDMS samples with Au of 0, 0.5, 1.0, 1.96, and 3.85 Au% in 1 gram of PDMS with their average output voltages.	50
B.1	Electronic components used in control system of our device	65
C.1	Electronic circuit used for constructing the ON-OFF switching system of our tapping device.	66
D.1	Signal data processing	67

List of Tables

3.1	Output voltage obtained from each peak during contact and separation between metal electrode and PDMS	31
-----	-----------------------------------------------------------------------------------------------------------------	----

Chapter 1

Motivation

The aim of this study was to investigate the fundamental mechanism of triboelectricity using metal-polymer and polymer-polymer contact electrification/tribocharging. The theory of contact electrification; i.e. the history, triboelectric effect, its consequences, and the available charge transfer mechanisms were vigorously studied before carrying out experimental works. This study has led to a discovery of a new mechanism, which is contrary to the all available contact electrification mechanisms in the literature. It is generally believed that the fundamental mechanism of electrostatic generation is a process that produces positive charge during contact between two materials and negative charge during separation in one complete oscillation, but after thorough investigation we realised that the phenomenon is really misunderstood.

Literature results have shown that researchers usually care about generating high output power only, but do not care about what *really* ignites the electricity, how is it generated and so on. In an attempt to deeply study the fundamental mechanism of the contact electrification and find answers to some controversial issues, we developed a mechanical tapping device suitable for testing triboelectric charge of all kinds of polymers or insulators at any given frequency. While carefully studying the effect we discovered and propose, contrary to the aforementioned theory on contact electrification mechanism, a new mechanism of charge

generation by contact electrification and electrostatic induction. The mechanism indicates a combination of both positive and negative charges during contact and a single positive or negative charge signal (depending on the initial charge polarity of the materials in contact) during separation, both of which generate charge induction in subsequent contact/separation just after the initial contact and separation. Certainly, people misconceive or intentionally neglect these observations because numerous data from literature have shown our observed signals, but to the best of our knowledge, no one could explain it.

Chapter 2

Introduction

2.1 Triboelectricity

Every person who has had the encounter of walking across a carpet, mat or floor cloth and felt an unexpected and annoying shock just after touching a metal doorknob, or noticed when a balloon is rubbed against hair it sticks to the hair, has experienced a phenomenon known as contact electrification or triboelectricity.

Triboelectricity is generated whenever two materials rub, slide or roll on each other; thus it is an electrostatic charge generated as a result of contact and separation between two identical or different materials, either metal-dielectric or dielectric-dielectric. Contact electrification (triboelectric charging) occurs as a result of charge transfer between surfaces of two materials after contact and separation [1–4]. It is a widely known physical process which happens in many natural and technological phenomena [5,6]. Generation of lightning, electrostatic charge in dust explosions caused by interactions between particles [5], the behaviour of sand storms [6,7], and volcanic plumes [8,9] are examples of naturally occurring phenomena [5–9].

In technology, it is applied in electrophotography (laser printing and photocopying), electrostatic coating with powders, electrets (found in many types of equipment e.g. acoustic transducers) and electrostatic filtration and separations [5–7, 10–12]. Figure 1.1 shows some examples of naturally occurring and technologically applied triboelectric effects. In Figure 1.1a,b wind strikes metal blades of a military helicopter while landing on the ground, and volcanic eruption generates lighting by causing ashes to propel into the sky [13]. Charge transfer is initiated after charge is generated when the wind blows and causes sand particles to collide with one another [14].

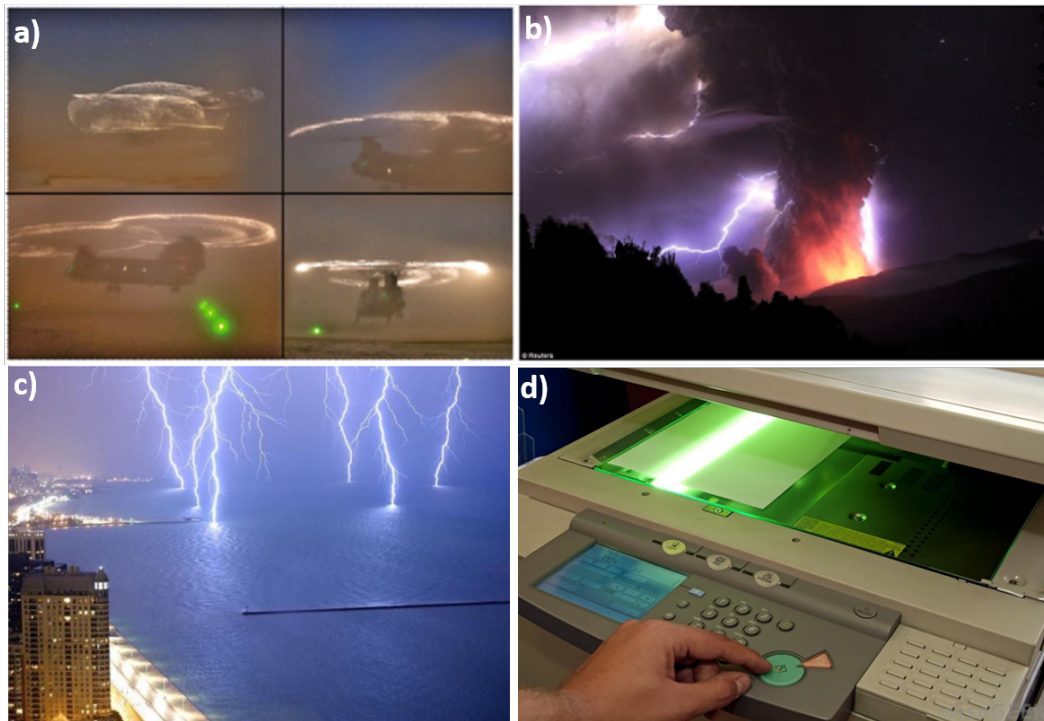


Figure 2.1: Naturally occurring triboelectric phenomena with dusty environments; (a) Countless small sparks due to grains of sand striking metal rotor blades of military helicopters while landing on the ground in deserts, popularly known as “corona effect” producing mega volts. (b) Incredible lightning flashes generated by volcanic eruption [13]. (c) Energy from hygroelectricity and lightning. (d) Technological application; xerography.

2.1.1 History of triboelectricity

This phenomenon of generating electric charge by contact and separation between materials is frequently called ‘contact electrification’ or ‘contact charging’, and when the materials are rubbed against each other it can be named ‘frictional electrification’, ‘triboelectrification’, ‘triboelectric charging’ or ‘tribo-charging’ [15]. The earliest experiments on triboelectricity were said to have been reported by one of the seven philosophers of early Greece [16], Thales of Miletus, over 25 centuries ago when he demonstrated electrostatic charge generation by rubbing two dielectric materials (amber and wool) [5, 10–12, 16]. Even though there are no written documents supporting the role of Thales in the discovery of this phenomenon, he is generally credited with it [10, 16, 17].

Triboelectricity is one of the most aged scientific research fields in the world. In the ancient past, due to its association with rubbing of material on amber, electrostatic effect was popularly known as the “amber effect” [17]. The term “electricity” is derived from the Greek word for amber “elektra” [18], and the word ‘triboelectric’ means ‘rubbing amber’ in Greek (which is a combination of two Greek words *tribo*, meaning to rub, and “amber”) [19]. Until the seventeenth and eighteenth centuries when various scientists made paramount systematic observations of electrostatic phenomenon, electrostatics was really a static topic.

William Gilbert, who was quite blistering about the “theoretical work” of early Greek scientists for conducting very few experimental work on static electricity [16], demonstrated that many other materials (which he called “electrics”) can generate electricity by rubbing; it is not only amber that has the ability to attract objects when rubbed [19]. Nowadays, Gilbert’s *electrics* and *non-electrics* (which are difficult to be electrified by contact) are called *insulators* and *conductors* [20].

In the early 18th century, another English scientist “Stephen Gray” discovered that when objects were united together by a metal “electricity virtue” could be transferred from one object to another [19]. He was an active experimentalist of electricity who conducted an experiment that led to the understanding of distinction between insulators and conductors [19, 20]. He realized that conductors

like copper or silver convey electricity, whereas insulators like silk or rubber do not [20].

In 1734, Charles Dufay classified electricity generated by friction into two types, namely; *vitreous*, which is created on crystals, glass, rock, wool, etc., and *resinous* produced on materials that are resinous like gum, rubber, paper or silk [10, 19]. Dufay was also the founder of the general principle that says “like charges repel while unlike charges attract each other, and that any force between charged bodies rely on the kind and amount of charge” [19].

Later, Benjamin Franklin introduced the terms “positive” and “negative” charges which substituted Dufay’s designations for vitreous and resinous electricity. He also made a proposal that caused the discovery of a theory “In an isolated or closed system, the algebraic sum of the positive and negative charges is constant”, popularly known as the *principle of conservation of charge* [19–21].

2.1.2 Triboelectric effect

Triboelectric effect involves the appearance of triboelectric charges with opposite signs at surfaces of the two different materials during and after contact. It can occur at solid-liquid, solid-solid or liquid-liquid interfaces [22–24]. In the case of dissimilar solids, which are originally zero-charged and usually at ground potential [22], it is generally thought that electrical charge is exchanged or transferred from one material to the other whenever they interact [23, 25]. However, Grzybowski and coworkers showed that two identical pieces of polymers (PDMS) can get (+) and (–) charges when they are contacted and separated [26]. As the two materials become oppositely charged, the surfaces obtain a net electric charge which forms electric field in between [22].

Being one of the most ubiquitous phenomena which can explain most of the static electricity generated in our daily life, triboelectric effect has recently been utilized as an effective means of harvesting enormous amount of mechanical energy and converting it into electricity for novel energy applications like chemical

sensing [27], charging portable electronic devices [28], sustainable power sourcing [29], light sensing [30], magnetic sensing [31] and other self powered systems [32–34], based on coupling between triboelectrification and electrostatic induction [33–36]. These types of power generating devices, called triboelectric nanogenerators (TENGs), are cost-effective, simple and robust for energy harvesting [33–38]. In TENGs, energy conversion process is achieved by periodic contact-separation (vertical or horizontal) mode based on charge polarization, or sliding mode [39] depending on in-plane charge polarization [40, 41].

2.1.3 Consequences of tribo-effect

Here, we briefly discuss some important consequences and hazards of triboelectricity. Despite its usage in technology, contact charging can also be a little menace to humanity; for instance, by causing troublesome electric shocks at homes and work places.

2.1.3.1 Important consequences

As mentioned earlier, triboelectrification has many advantages in technology and few disadvantages such as damage to electronic components. It is applied in many areas of technology like biotechnology for study and manipulations of DNA using electrophoretic and dielectrophoretic forces [42], space applications, electrostatic precipitation and coating [42], pharmaceutical dispersal devices e.g. dry-powder inhalers [43, 44], electrostatic separation [45], xerography [46] and digital printing by charging of toner particles [47].

2.1.3.2 Hazards triggered by triboelectric effect

Tribo-effect can create static charge accumulation and their successive discharge, known as electrostatic discharge (ESD), on material surface which can be very harmful in explosive and flammable environments [48]. When the accumulated

charge turns out to be adequately high in such environments, in tens of kilovolts level, it causes gas failure which results in sparks [6, 48]. Lightning and other natural emissions are often regarded as hazardous to every creature. Electrostatic charges are sometimes discrete and undetectable, that is why materials that are seemingly safe and benign to naked eyes keep large quantities of charge [10]. Some of the numerous incidents that happened in the past are; several accidents within the period of 1950-1970 in many industries like chemical, defense and petroleum [49]. In order to avoid Electrostatic Discharge (ESD) effect in electronic industry, some danger prevention measures like the use of Personal Protective Equipment (PPE) [50], standard electrostatic test methods, and shielding packaging for sensitive parts protection from ESD damage when in an unrestrained environment, are taken [51].

2.1.3.3 Some examples of energy harvesting devices

Harvesting mechanical energy from our surroundings is a potent perspective for obtaining cost-effective, maintenance-free, clean, sustainable, and green power source for wearable [52], portable and wireless electronics [53, 54]. Owing to the increase in anxieties about the climatic change and energy crisis, renewable energy technologies have received very much attention. Now, devices that are usually powered by batteries are in serious need of smaller or similar size sustainable energy sources, because the development of nano/micro size electronics has decreased power consumption which enable them to be powered by small scale energy harvested from ambient environment [55]. Nowadays, researchers are developing self energy driven shoes for harvest energy from human walking and converting it into electricity for charging portable electronic devices like cell phones [56, 57]. Figure 2.2 shows some triboelectric nanogenerators used for harvesting energy from water-flow, and wind energy from human mouth. Other examples of TENGs are shown in Figure 2.3.

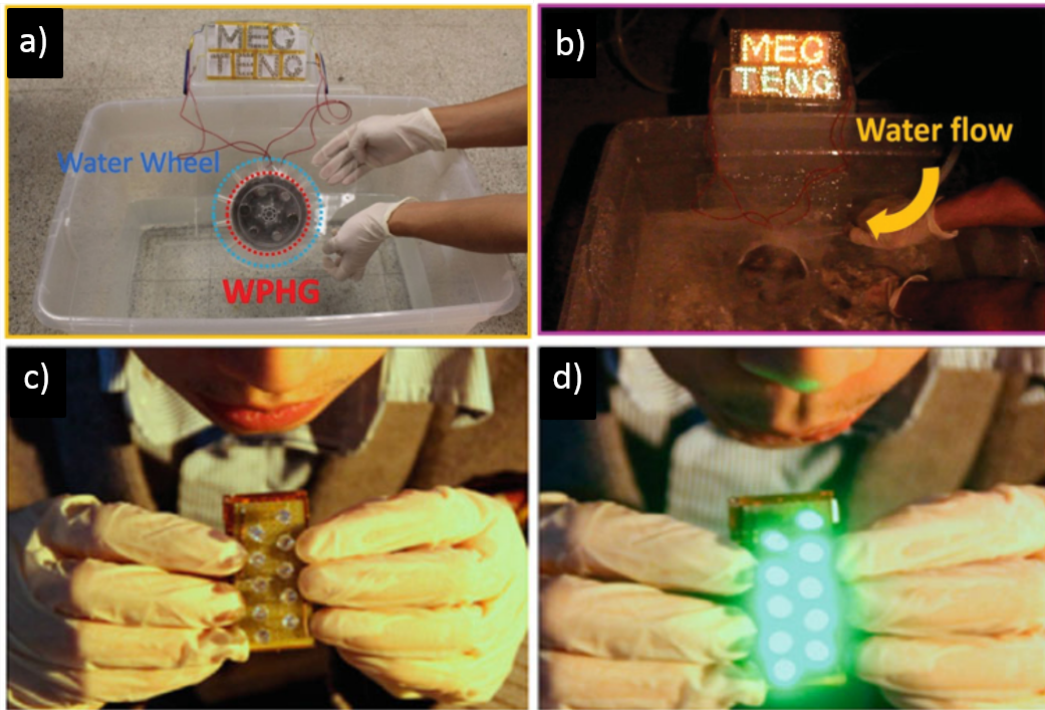


Figure 2.2: TENG used for harvesting water-flow energy in the water: (a) before working and (b) after working (adapted from [58]). (c) TENG was used for harvesting wind energy from human mouth (d) to drive 10 LEDs [59].

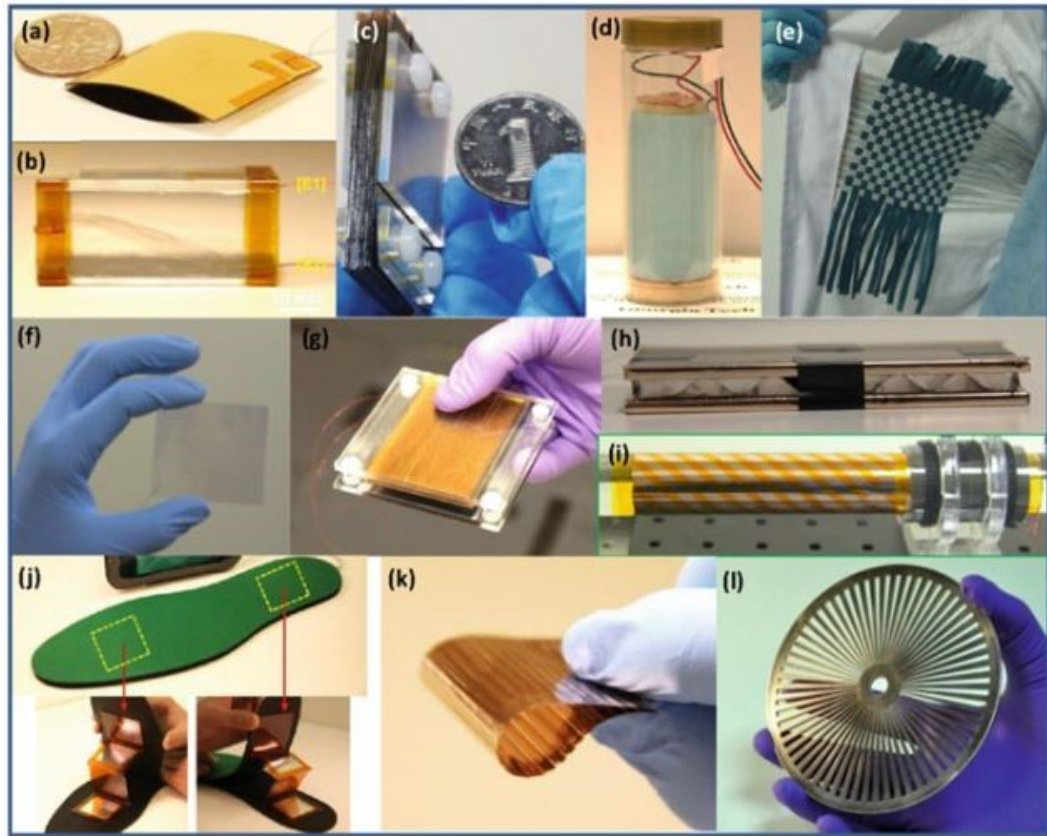


Figure 2.3: Other examples of energy harvesting devices: (a) Finger tapping energy. (b) Air-flow energy. (c) Sliding energy. (d) Enclosed cage for harvesting energy in water. (e) Textile for harvesting body motion energy. (f) Touch pad. (g) Foot or hand pressing energy. (h) Water impact energy. (i) Cylindrical rotation energy. (j) TENG In-sole for harvesting walking energy. (k) Harvesting sliding energy. (l) Rotation energy from disc shape [60].

2.2 Theory of the Charge transfer mechanisms

Despite the fact that triboelectric effect has been known and applied for many years, there is still lack of understanding of the basic mechanisms [61–66]. For instance, the **kind of charge carriers** or material that is being transferred/exchanged from one surface to another during contact and separation is not clear. Many researchers have classified the tribo-charge transfer mechanisms

into three fundamental processes: **electron**, **ion**, and **material** transfer mechanisms [6, 10, 67–72]. Some groups further investigated the happenings on tribo-charged surfaces and concluded that there are other possible processes involved, which include bond-forming, bond-breaking and chemical changes [1, 12, 69–73].

In the following sections, the above mentioned three fundamental mechanisms are discussed based on interactions involving polymeric (or insulating) materials. Contact electrification between two metals is different from the one involving only polymers or metal-polymer, it is well understood [5]. Tribo-charging of metals occurs as a result of transfer or exchange of electrons between them, due to difference in their work functions. Work function is the energy needed to remove an electron from the surface of solid material, usually metal.

The difference in the Fermi level (or work functions) of metals let electrons flow from the metal with lower work function to the one with higher work function and cross the boundary until their chemical potentials reach thermodynamic equilibrium [15, 22]. Figure 2.4 depicts a metal-metal surface charge transfer; where “Metal A” with lower work function ϕ_A (higher Fermi level “ E_{F_A} ”) becomes positively charged after making contact with “Metal B” of higher work function ϕ_B (lower Fermi level “ E_{F_B} ”). The transfer of electrons generates potential difference “ V_c ” between the surfaces of the metals:

$$V_c = \frac{\phi_B - \phi_A}{e}, \quad (2.1)$$

where e is the electronic charge ($e = 1.6 \times 10^{-19}$ C) [15, 22, 70].

Charge transfer also depends on the effective capacitance of the interface between materials in contact, which is related to their state densities and dielectric constant at the interface. If the charge transfer at the interface is similar to charging of a capacitor with capacitance C , then the process should involve relaxation time “ τ ” for it to reach equilibrium condition [22].

$$\tau = RC = \rho\varepsilon, \quad (2.2)$$

Where R is the electrical resistance, ε the permittivity at the interface and

ρ resistivity. In case of highly insulating materials, τ turns out to be extremely large which can avert the attainment of equilibrium state. Charge recombination cannot fully arise if one or both of the materials are insulators, thus the materials hold back their charge after separation [22].

The amount of total charge “Q” transferred after contact and separation can also be determined using the following equation:

$$Q = C_0 V_c, \quad (2.3)$$

where Q is the total charge and C_0 capacitance of the system related to contacting materials.

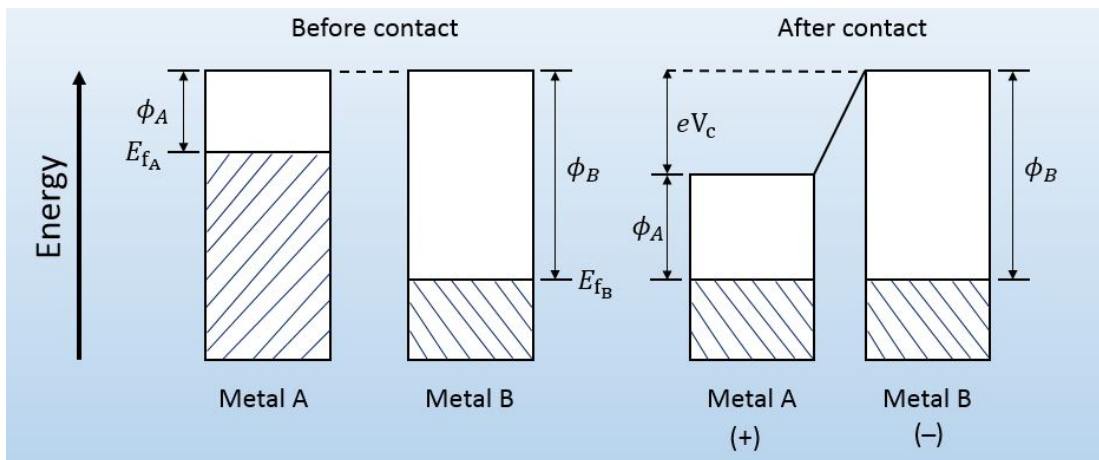


Figure 2.4: Surface charge transfer between metal-metal contact.

2.2.1 Electron transfer

In the late twentieth century, Lowell and Rose-Innes [72] made a classical review on contact electrification that is full of perceptive insights into the field, more especially about the mechanism of electron transfer. For contact that involves at least a metal or a semiconductor, electron dominates charge transfer in the system. If both materials are polymers (or insulators), then charge carriers alone cannot give an insight about the basic charge transfer mechanism, chemical nature of functional groups need to be examined as well [68, 70]. In theory valence and

conduction bands of insulators may have small amount of charges, but according to Lowell *et al.* the charges are negligible in experiment if the surfaces of the bands contain some electrons beyond and beneath Fermi level of metal [72].

Figure 2.5 shows a model for metal-polymer charge transfer, with z as the intermolecular distance between them after contact where equilibrium is established, E_F the Fermi level of the metal, ϕ_M is the work function for metal and ϕ_P for polymer. HOMO is the highest occupied molecular orbitals and LUMO is the lowest unoccupied molecular orbitals. The equilibrium is attained immediately after contact by either replenishing or emptying the electronic orbitals near work function of the polymer, ϕ_P [15].

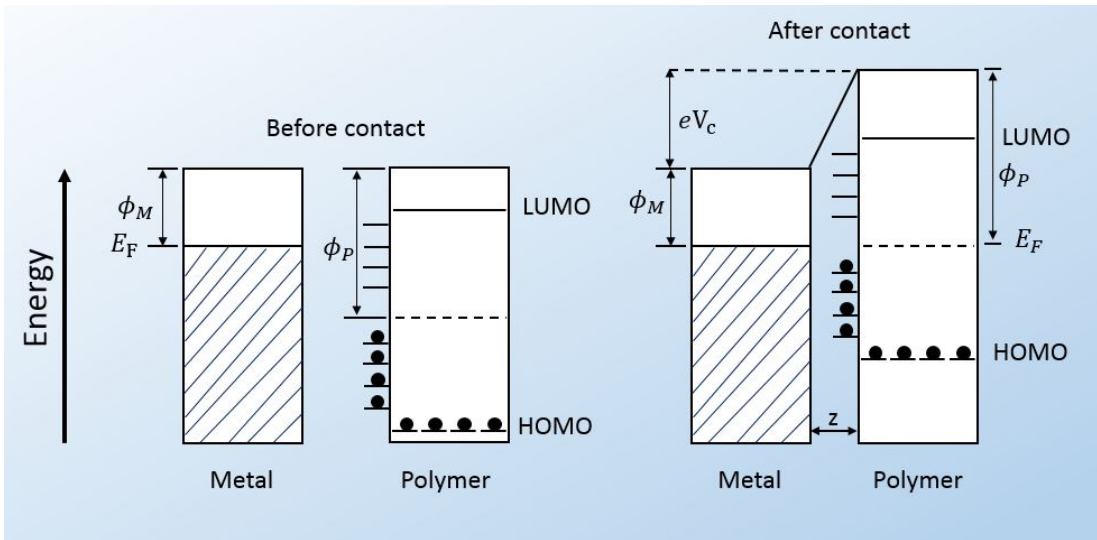


Figure 2.5: Surface states of metal-polymer, before and after contact.

Owing to the absence of free electrons in polymeric or insulating materials, it is still unclear how electron transfer occurs during contact. In insulators, electrons are sparsely arranged due to a large band gap that separates valence and conduction bands which prevents them from flowing [14]. In order to solve the problem of free electrons and pave a way to charge transfer in dielectrics, some researchers [71,72] provided numerous models some of which are similar to metal-polymer contact model with limited flow of electrons in the system [15]. Lowell and Rose-Innes [72] mentioned that, according to thermodynamic equilibrium theory, the charge transfer mechanism between a metal and a dielectric material

in triboelectrification occurs as a result of electron transfer from the metal to the dielectric material (see Figure 2.5 for more detail).

It is generally believed that electron energy levels are not in bulk but present only at the surface of material, as shown in Figure 2.6 where electrons flow from the filled surface of polymer 1 with work function ϕ_{P_1} to the empty space on the surface of polymer 2 with work function ϕ_{P_2} until equilibrium state is reached after contact between them. Charge transfer causes equal Fermi energy level “ E_F ” between the two polymers with change in work functions (ϕ_{P_1} and ϕ_{P_2}) and potential difference [15].

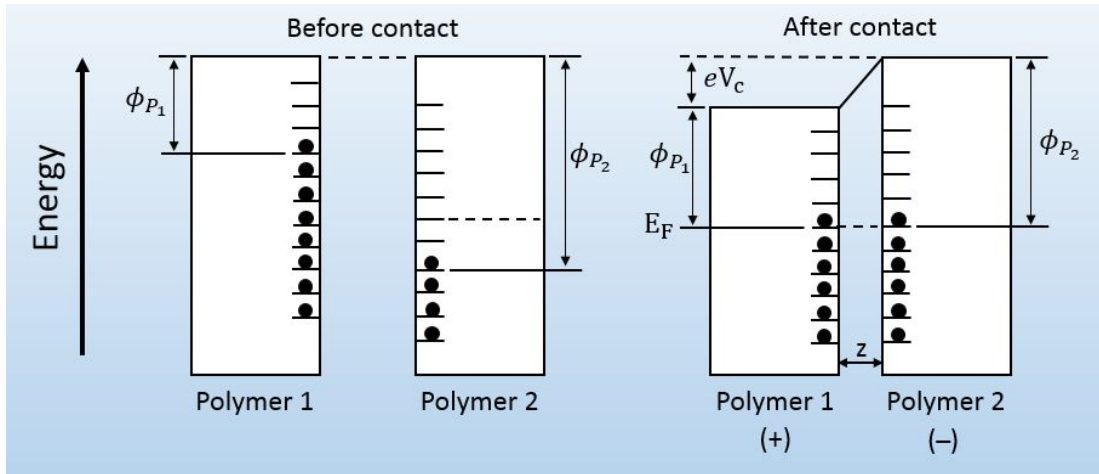


Figure 2.6: Surface states of polymer-polymer, before and after contact.

Harper [74] was said to have gathered opinions of some scientists about the conflicting perspectives on charging polymers (or insulators), whether static electricity is generated by ion, electron or both. Loeb claimed that charge carriers are generally electrons, Montmometry said charge carriers are always electrons and Henry thought that the topic was still open for discussion [10]. Recently, new interests have been found on the argument; Baytekin *et al.* used surface characterization techniques to study the surface composition of the tribo-charged surfaces at nanoscale and concluded that “it is not only transfer of electrons, ions or both that are responsible for contact electrification between the surfaces of materials, it involves spatially inhomogeneous material transfer” [67].

2.2.2 Ion transfer

As earlier stated some researchers believe that contact electrification may involve ion transfer or exchange between surfaces of materials [25, 71, 72, 75, 76]. Whitesides' group [76] proposed ion transfer mechanism and experimentally proved that; for polymers containing mobile ions there is transfer of ions during contact. These kinds of insulating materials have bound ions and counter ions with opposite charge polarities that allow the transfer of ions after contact [76]. For metal-polymer contacts only very few ion transfer models are proposed [71].

In the twentieth century, Mizes and co-workers showed that by doping some polymers with ions it is possible to transfer ions from polymer to the metal [25]. Based on their findings some researchers believed that ion transfer is definitely among the general charge transfer mechanisms [74, 76].

2.2.3 Material transfer

In 1967, Harper [74] mentioned that contact electrification may also involve material transfer in the process. Eleven years later, Salaneck *et al.* validated how material is being transferred between two contact surfaces (metal-polymer or polymer-polymer) using non-destructive spectroscopic analysis [77]. Salaneck and co-workers also reported that transfer of material decreases as the number of contacts increases subsequently and based on that Lowell assumed that material transfer would not continue if contact is repeated forever [78]. This implies that material transfer is not the main cause of contact electrification.

The transfer involves just pieces of materials on both of the tribo-charged surfaces at nano/micro scales. These pieces of materials have high possibility of taking away charge due to bonds breaking in the contact process [5]. Baytekin *et al.* validated that contact charging involves both material and charge transfer. They further demonstrated, using polymer films of different compositions, that the charges produced on each surface are both positive and negative (surface

charge mosaic) [12]. Also, our recent XPS (x-ray photoelectron spectroscopy) surface analyses of metal and PDMS after contact have shown that material transfer occurs due to bonds breaking (see results and discussion in chapter 3).

2.3 Triboelectric series

Triboelectric series, named by Shaw in 1917 [5], is a semi-quantitative or qualitative arrangement of materials based on their tendency to gain either positive or negative charge on contact with other materials [70, 76, 79]. After contact, the material nearer to the top (positive end) of the series will gain positive charge while the one nearer to the bottom (negative end) will gain negative (see Figure 2.7) [76, 80]. The published list in Figure 2.7 is an example of triboelectric series of some materials, adapted from [10] and [76]. For example glass which is very close to the top gain positive charge when contacted with Teflon (PTFE) which is at the extreme end also develops negative charge.

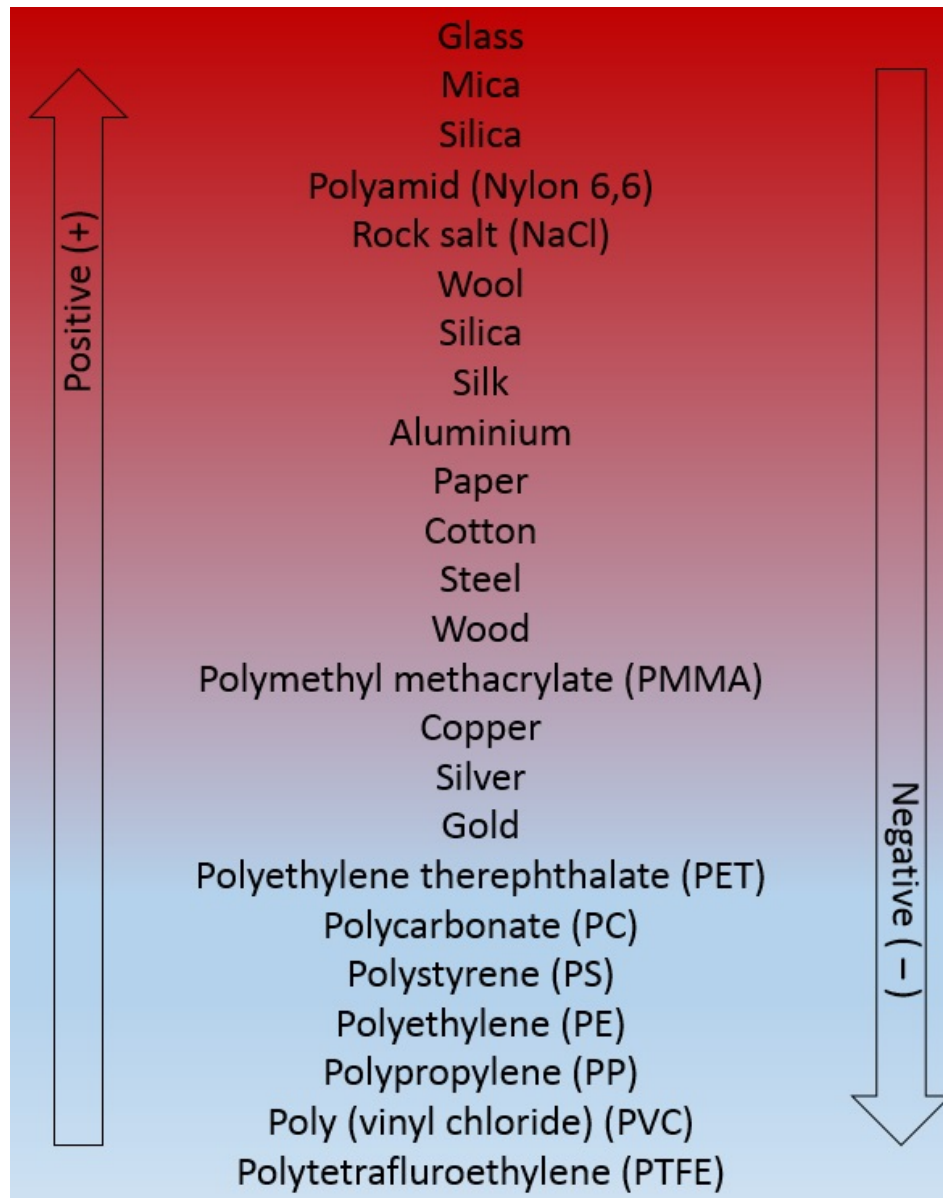


Figure 2.7: Triboelectric series of some materials, adapted from [10] and [76].

Chapter 3

Contact electrification and tribocharge generation for metal-polymer and polymer-polymer interactions

3.1 Introduction

Concerns over the controversy regarding the mechanisms of contact electrification between metal-polymer and polymer-polymer have led us to a thorough investigation of the fundamentals of triboelectricity. In order to answer the questions; how electricity is generated from contact effect, what ignites it, the chemistry and physics behind it, etc., we developed a tapping device for detailed analysis of the basics of contact electrification at low, moderate, and high frequencies.

In this study we discover and propose a new mechanism of charge generation by contact electrification and electrostatic induction. We realised that people generally operate their tapping devices at high frequencies while neglecting the low

and moderate frequencies, thus not being able to observe the fundamental mechanism of triboelectricity or failing to report the real happenings during contact and separation of materials. In order to clarify the issue, we first discussed the available contact electrification mechanisms in the previous chapter, and here our proposed mechanism is discussed based on experimental evidence in the following sections.

Before proceeding to our proposed mechanism we discuss some literature results that technically verify our findings, but nobody could explain the contact and separation signals in their literature data. They generally focus on the electrical performance of their tribocharge generating devices only. Figure 3.1 shows some results with two different categories of peaks, as in our mechanism, indicating combination of induction and contact peaks from contact charging and a single peak from separation (see section 3.4 for more information). In Figure 3.1a, they explained *only* the contact peaks (according to our own mechanism) as their contact and separation peaks while neglecting *the real separation peak* [81]. Figure 3.1c depicts PDMS-PDMS contact results by Yu *et al.* showing contact signals highlighted as pressing and releasing, which means contact and separation, while neglecting *the actual separation signal* with lower output current density [82]. Similar thing is shown in Figure 3.1d from kapton-kapton contact and separation. More literature results are shown in Figure 3.2 with enlarged view of contact and separation signals indicating a combination of positive (**1**) and negative (**2**) peaks from contact and a single peak (**3**) from separation (Figure 3.2e), which we already explained in our mechanism but still pending in the literature. These results have shown that researchers have not figured out what really happen in contact electrification between identical or dissimilar materials. People might not care about the real mechanism because electricity is generated anyhow, but it is very crucial in understanding some contentious issues. Our proposed mechanism is distinctly discussed in section 3.4.

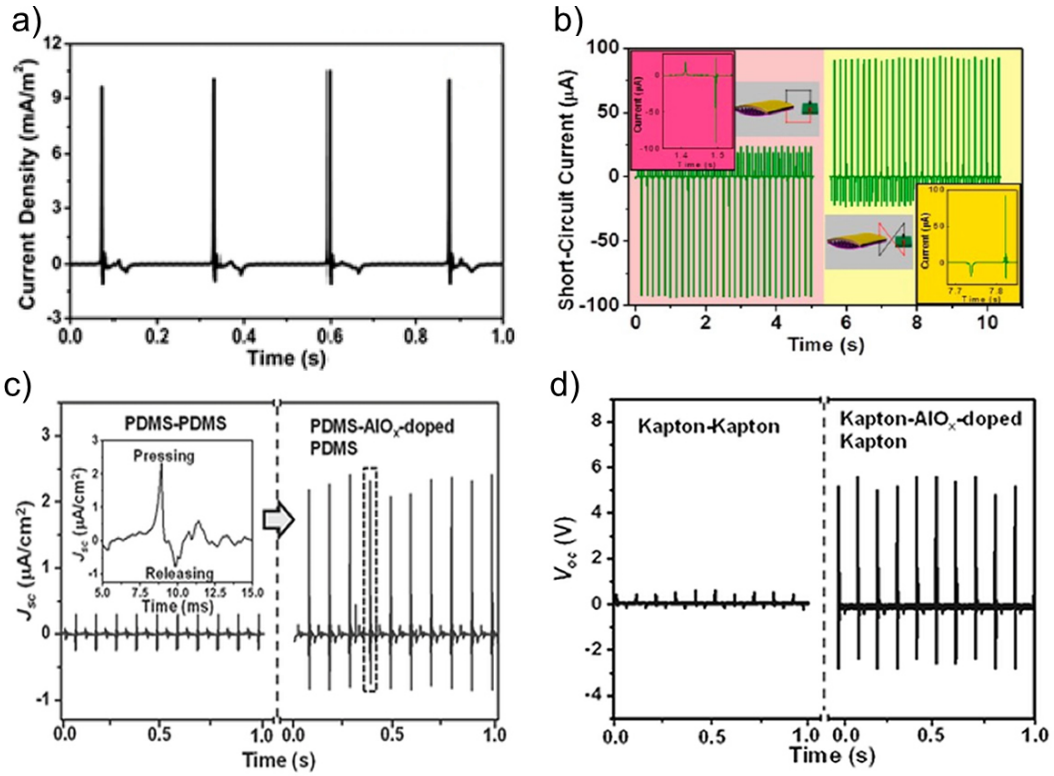


Figure 3.1: Unexplained literature results showing our proposed mechanism: (a) Current density result adapted from [80], showing contact and separation signals separately. (b) output voltage results of triboelectric sensor indicating peaks from contact and a peak from separation [29]. (c) PDMS-PDMS and PDMS with doped AlO_x contact and separation, (d) kapton-kapton and kapton- AlO_x doped contacts [82].

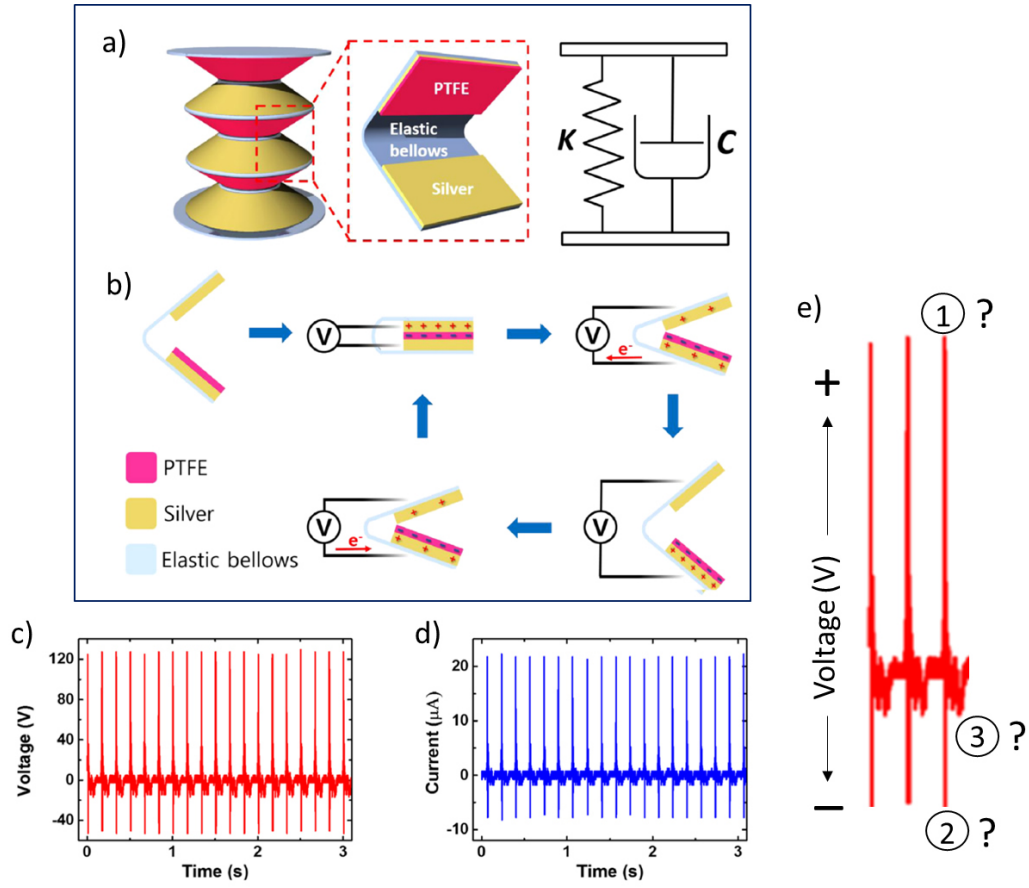


Figure 3.2: More literature results practically showing our proposed mechanism: (a) The structure of elastic triboelectric nanogenerator. (b) The working mechanism of the TENG. Output performance of the device; (c) voltage output, and (d) current output. (e) Enlarged view of the first three contact and separation signals of (c), technically verifying our proposed mechanism by showing a combination of positive (1) and negative (2) peaks from contact and a single peak (3) from separation but not explained in the literature [83].

3.2 Experimental Section

3.2.1 Polymer film preparation

Polydimethylsiloxane (PDMS) samples were prepared by mixing and curing methods [84]. The films were produced by thoroughly mixing elastomer and cross-linker or curing agent (purchased from Dow chemical company) at 10:1 weight ratio [84, 85] for about 30 minutes and waited for 2 hours at the ambient laboratory environment before heating. The mixture was then heated in an oven under vacuum at 65 °C for 10 hours. After the removal of PDMS films of different thicknesses from the oven, samples were smoothly laid on the surfaces of Al and Cu SEM stubs of three different diameters (6, 12 and 18 mm, respectively) for contact and experiments. The metals (Al and Cu) were used as supporting and contact electrodes in the experiment. All necessary measures to avoid air interference between metal and polymer were taken. PTFE and the rest of the polymers used were ordered from McMaster. The samples were systematically investigated and demonstrated as instantaneous source in order to measure their output power, open circuit voltage and short circuit current (see next subsection).

At the beginning of this study, the polymers used were only polydimethylsiloxane (PDMS) and polytetrafluoroethylene (PTFE). We later used polysulfone (PSU), polyvinyl chloride (PVC), polypropylene (PP), kapton, acetate, Polyethylene terephthalate (PET), polycarbonate (PC), and Nylon for deeper understanding of triboelectric effect and verification of our hypothesis.

3.2.2 Voltage and current measurement

In order to deeply investigate contact electrification at any frequency, we developed a reliable and virtually noise-free mechanical tapping device (Figure 3.3) and designed its control system using microcontroller (Arduino Nano) and some additional electronic components (2N3904 NPN transistor, 1N4007 diode, 1K and

10 K resistors). The codes used for running the tapping device are shown in Appendix A. The control system, the schematic used for building the whole system are shown in Appendix B and C. The device work on horizontal contact mode, with one sample fixed and the other making periodic motion. For instance, in the case of metal-polymer contact all polymers were static on a metal electrode and another metal electrode was making the oscillatory tapping motion.

We measured the open circuit voltage and short circuit current of the polymers using our tapping device at 1, 3, 10, 15 and 20 Hz, respectively. All data were taken using digital oscilloscope (Owon SDS7072 70 MHz, 2+1 Channel, 1 GS/s) with P4100 Series probes (100:1/100 MHz, Input voltage 2KV DC + AC pk, P4100 series High voltage probes), low-noise current preamplifier (SR570 Current Preamplifier) and transferred to computer for processing. The voltage and measurement setup are designed in Figure 3.4 (see Appendix D for data processing). 4189 Treacable Humidity/Thermometer-Control company was used to examine the effect of humidity and temperature on the output power throughout this study. The humidity recorded during this analysis fall in the range 13 to 35%, all measured using the above mentioned humidity meter.

Although there are some results taken from single electrodes, we generally used two channels of oscilloscope to take data from both electrodes simultaneously (base and metal electrodes), not the traditional way of taking data, i.e. connecting one electrode to ground and the other to current/voltage measuring device. In order to have full insight of the fundamental mechanism of contact electrification, the two oscilloscope channels were both connected to ground throughout the experiments to observe good signals from both metal and base electrodes. Figure 3.3a shows how probes 1 and 2 are connected to the base and metal electrodes (contact area). The red crocodile clip is the one connecting base electrode to the oscilloscope channel 1 and the black crocodile clip is the one connecting metal electrode to oscilloscope channel 2.

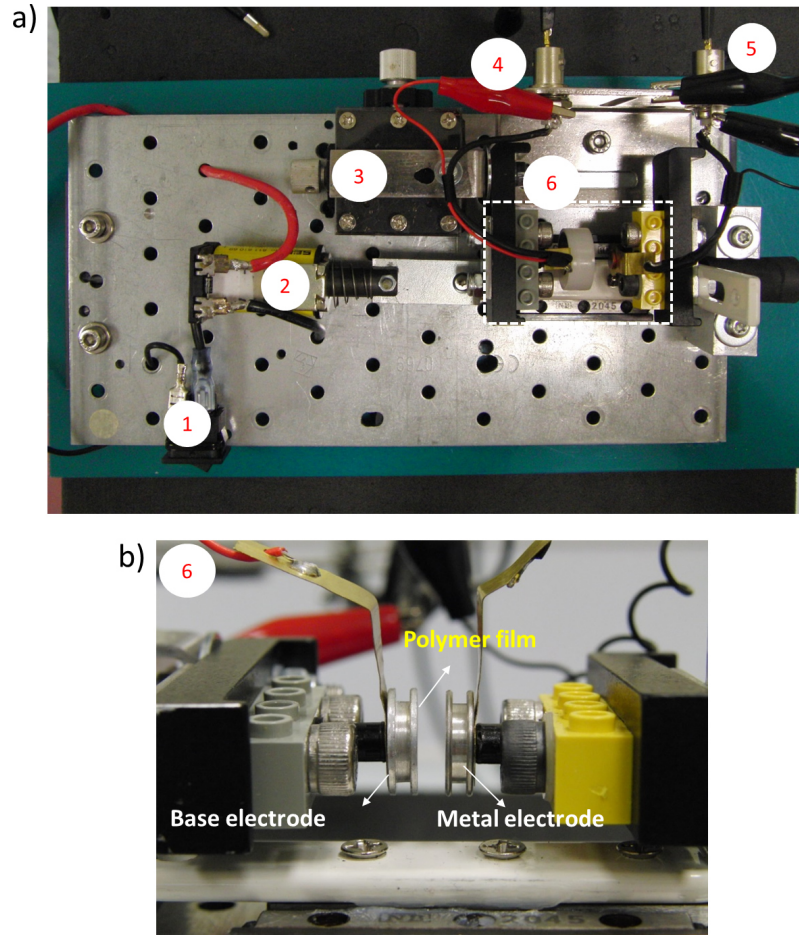


Figure 3.3: Mechanical tapping device used for electrical characterization of the polymers using contact electrification. (a) Top view of the device; (1) ON-OFF switch, (2) solenoid, (3) XY positioner, (4) probe 1 connected to base electrode, (5) probe 2 connected to metal electrode, and (6) contact area . (b) side view of the contact area.

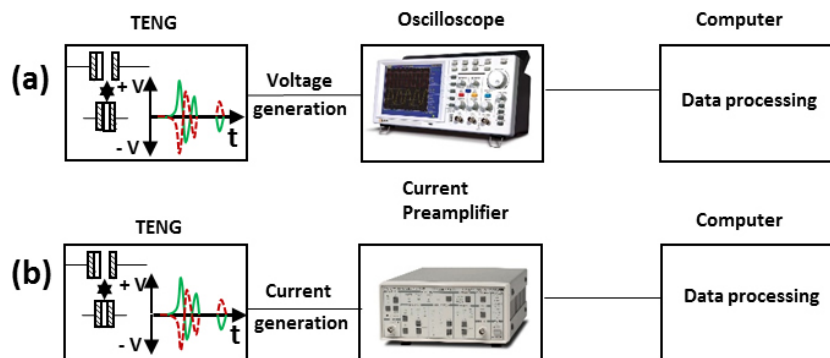


Figure 3.4: Measurement setup for the experiment: (a) Output voltage measurement. (b) Short circuit current measurement.

3.2.3 Surface characterization

To verify whether there is material transfer at the surface of materials after contact or not, pieces of PDMS and metal (Al foil) were analysed using XPS after a very soft contact and separation. The XPS used in this study was; Thermo XPS, Model: K-Alpha - Monochromated high performance XPS spectrometer). Also, to verify the existence of Au nanoparticles in PDMS-AuNp doped samples scanning electron microscopy (SEM) images of the pure PDMS and all AuNp doped samples were taken using FEI QUANTA 200F scanning electron microscope at high voltage (HV) of 10.0 KV, spot size of 3.0 and 100 microns. The samples were first coated using PRECISION ETCHING COATING SYSTEM with carbon of density 2.25 g/cm^3 and acoustic impedance of 2.71 ohms to make the surfaces conductive and obtain high resolution images.

3.3 Results and discussions

From our results, we have discovered that in every complete cycle of triboelectricity; contact gives both positive and negative potential signals in a complete oscillation while separation gives a separate (+) or (-) peak only. However, literature always indicate that contact gives only a positive peak while the separation gives only a negative in a complete cycle. According to our discovery when two materials (dielectric-dielectric or metal-dielectric) come in contact with each other capacitive charge induction occurs between them which gives rise to electron transfer between the two materials. Obviously, literature studies misinterpret these observations. While in contact back flow of electrons occur from acceptor to the donor (now in need of electrons) which results in positive and negative peaks. This happens as a result of tunnelling of electrons between the surfaces of the materials in contact [71, 72]. The separation part also gives a different peak which is either positive or negative alone depending on the triboelectric charge of the material. We have tested our materials several times and observed similar behaviour. The study was further elongated to different kinds of polymers and

homogeneous contact and separation effects were observed. Here we discuss our experimental results, based on which we designed and proposed a new mechanism in the next section.

Alteration of the tapping frequency led us to perceive that the mechanism of contact electrification (explained in section 3.4) gives something different from what has been in the literature for so long. We noticed that at low frequency the separation signals begin to appear, while gradually increasing the frequency the separation peak moves towards the contact peaks (positive and negative) and finally leave no gap at some certain high frequency. Figure 3.5 demonstrates the results acquired from contact and separation of metal electrode with PTFE and PDMS at low, moderate and high frequency (1, 5 and 15 Hz). As the tapping frequency increases from 1 to 5 Hz, for both PDMS and PTFE contact and separation with metal, contact output voltage signals increase and separation signal moves closer to the contact peaks. At high frequency of 15 Hz, for both polymers, single peak each for contact/separation with induction is observed.

At 1 Hz a delay of about 0.5 seconds was observed between the contact and separation peaks due to low tapping force which keeps the separation a bit far from the contact peaks. By gradually increasing the frequency the separation peak draws closer to the contact peaks, as seen in Figure 3.5 (c), until it completely leaves no distance between the contact and separation (Figure 3.5d) due to high tapping frequency. This implies that from the experimental results it is not only PDMS, which is widely used by experimentalist and has piezoelectric properties as well, that behaves according to our proposed mechanism.

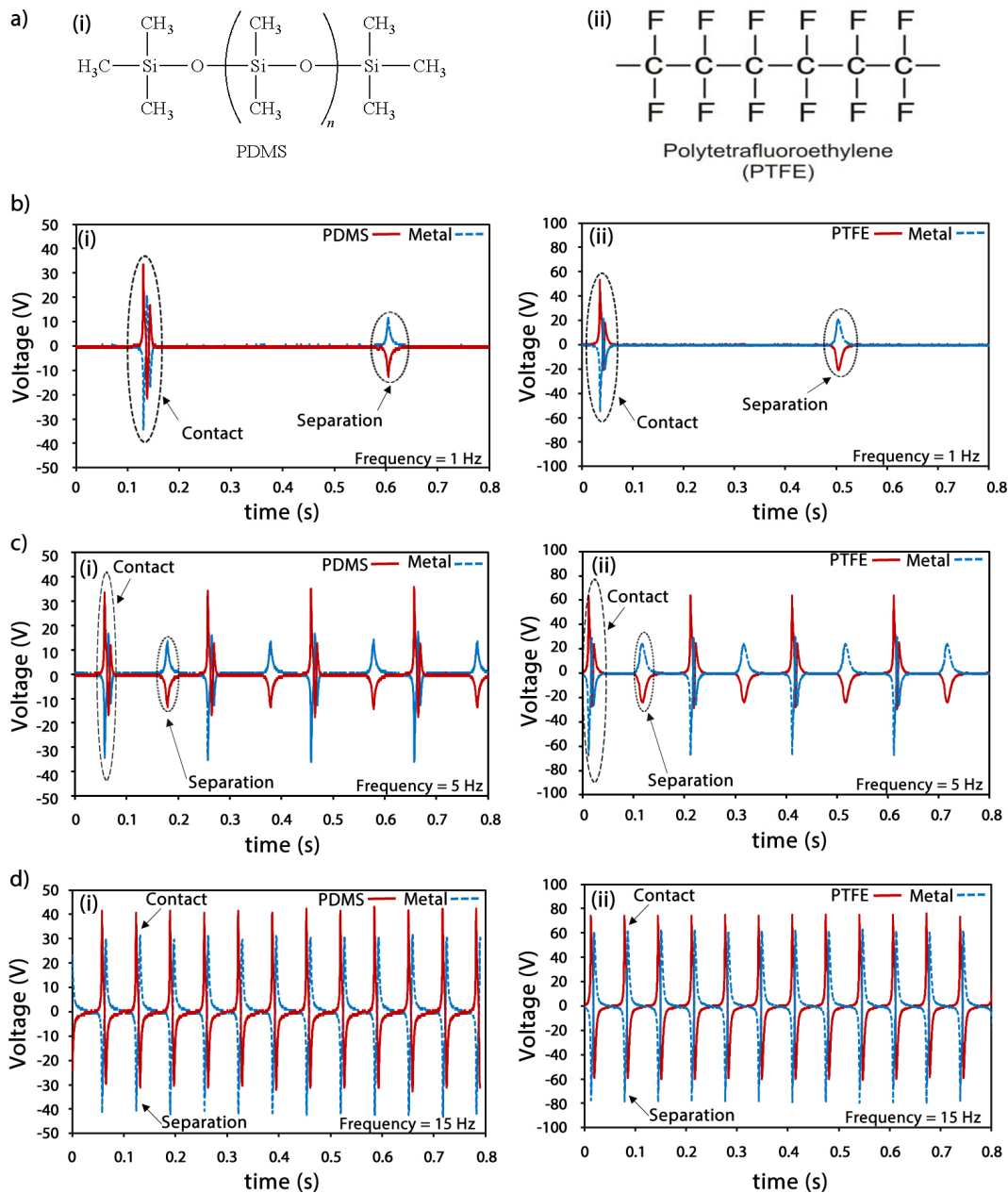
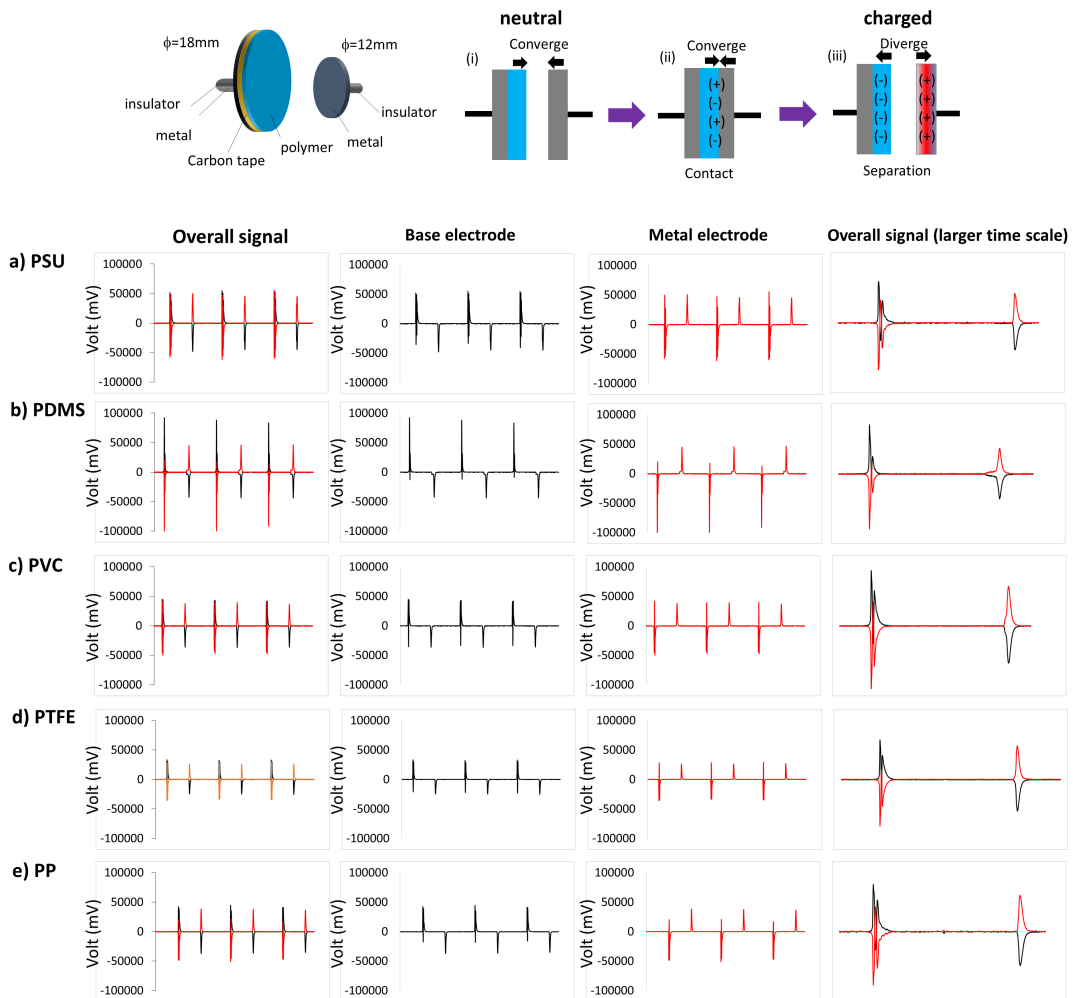


Figure 3.5: Contact and separation peaks obtained from interaction between 12 mm diameter aluminium metal and two different 18 mm diameter polymers (PDMS and PTFE) at low, moderate and high frequencies. a) Chemical structures of; (i) PDMS and (ii) PTFE. (b) At low frequency of 1 Hz separation appears to be far from the contact peaks (i) PDMS and (ii) PTFE. (c) As the tapping frequency increases to 5 Hz, for both (i) PDMS and (ii) PTFE, voltage signals increase but separation moves closer to the contact peaks. (d) At high frequency of 15 Hz, for both (i) PDMS and (ii) PTFE, single peak with induction combined is observed for each contact/separation.

More results of metal-polymer contacts are shown in Figure 3.6 with PSU, PDMS, PTFE, PVC, PP, kapton, acetate and PET. All the results show negative charge from polymers, and positive from metal electrode. However, Figure 3.7 shows some results that give opposite of the above mentioned results by showing positive from polymers (PC and Nylon) and negative from metal electrode. These results and the numerous data seen in the literature have verified the consistency of our mechanism of contact electrification and tribocharging based on metal-polymer and polymer-polymer contacts. All our polymers show similar behaviour to those in triboelectric series (Figure 2.7).



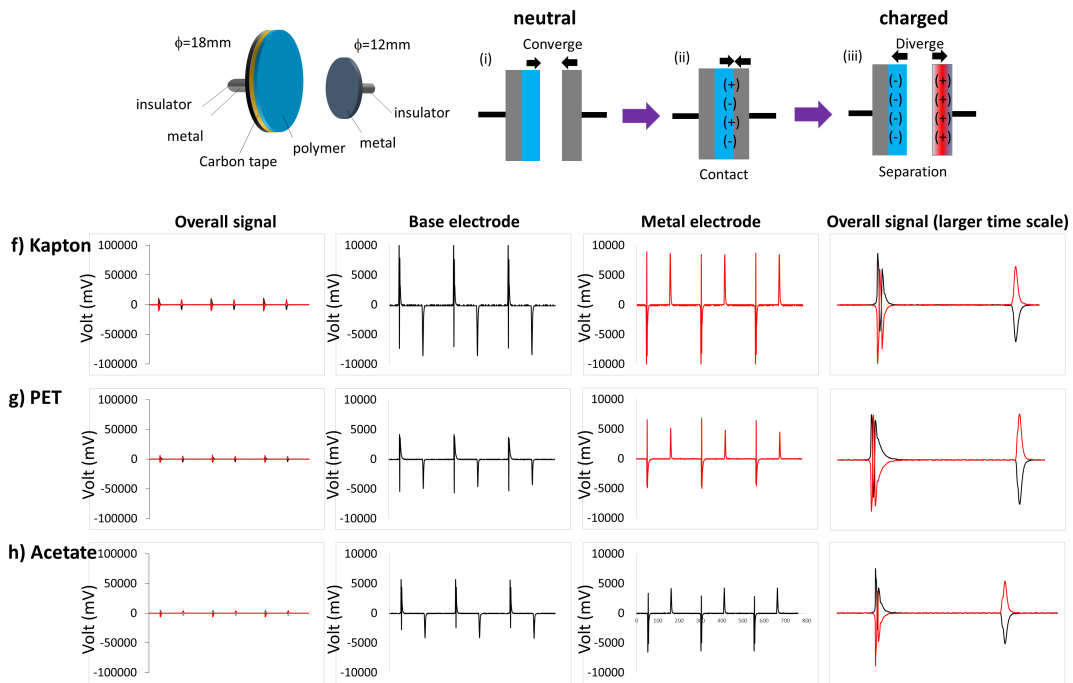


Figure 3.6: More results of interaction between 12 mm diameter aluminium metal and eight different 18 mm diameter polymers at low frequency for verification of our proposed contact electrification mechanism. a) PSU, (b) PVC, (c) PDMS, (d) PTFE, (e) PP, (f) Kapton, (g) PET, and (h) acetate.

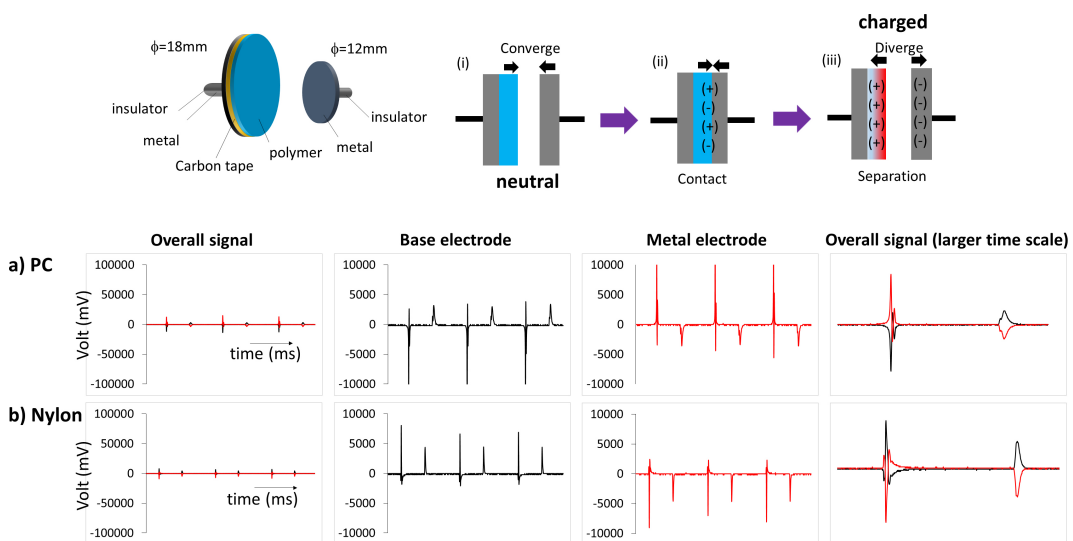


Figure 3.7: Signals showing positive charge from interaction of metal with (a) PC and (b) Nylon at low frequency.

Figure 3.8 illustrates detailed information of contact, separation, convergence induction (I_c) and divergence induction (I_d) on both materials during and after contact between aluminium metal and PDMS. The figure also indicates a clear picture of the overall event in contact and separation with all kinds of polymers. The amount of voltage obtained from each peak is also listed in Table 3.1.

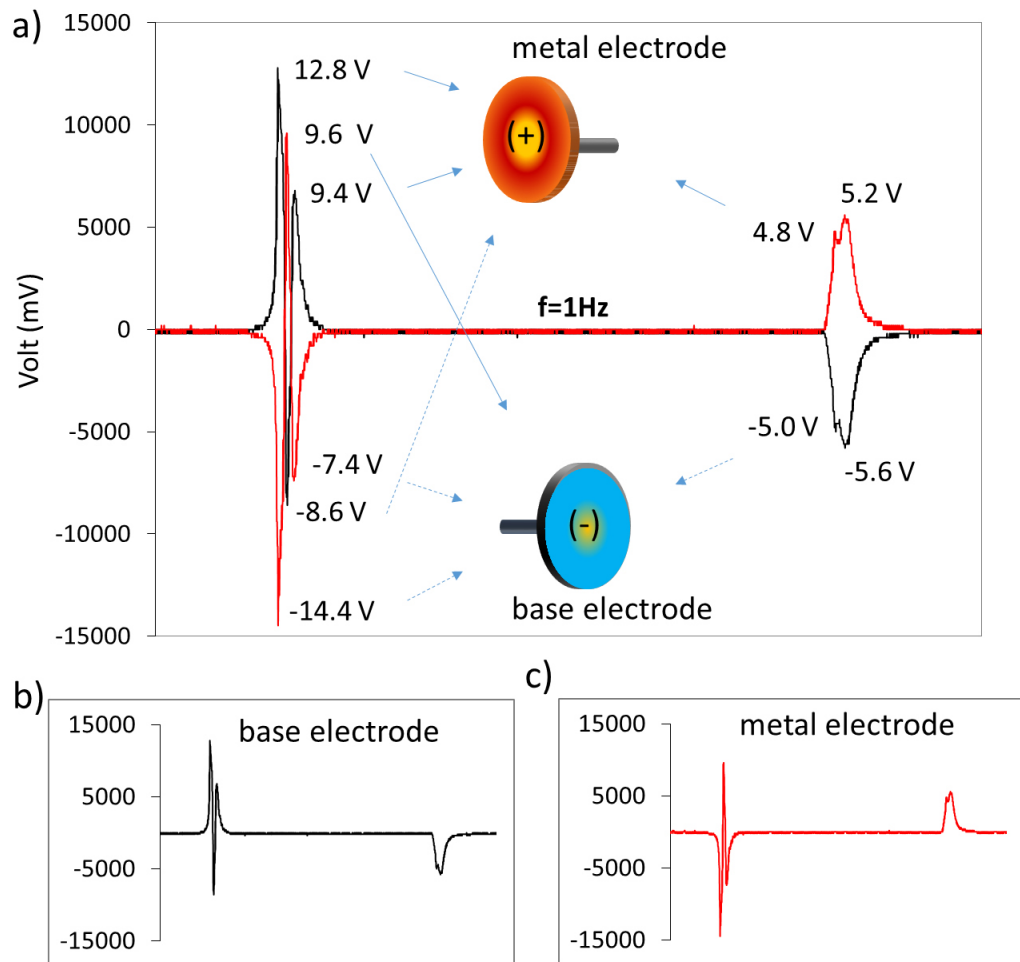


Figure 3.8: Detailed information of the contact and separation between PDMS and aluminium metal, clearly showing CE, SE, convergence and divergence induction (I_c and I_d) on both materials during and after contact. (a) Overall signal (b) Signal from base electrode (c) Signal from metal electrode.

(I _c) _{base}	(I _c) _{metal}	(CE) _{base}		(CE) _{metal}		(I _d) _{base}	(I _d) _{metal}	(SE) _{base}	(SE) _{metal}
		(+)	(-)	(+)	(-)				
14.4 V	12.8 V	9.6 V	7.4 V	9.4 V	8.6 V	5.0 V	4.8 V	5.6 V	5.2 V

Table 3.1: Output voltage obtained from each peak during contact and separation between metal electrode and PDMS. (I_c)_{base}: Induction signal for base electrode at the contact. (I_d)_{base}: Induction signal for base electrode at the separation. (CE)_{base}: Contact electrification signal for base electrode during contact. (CE)_{metal}: Contact electrification signal for metal electrode during contact. (SE)_{base}: Separation signal for base electrode during separation. (SE)_{metal}: Separation signal for metal electrode during separation.

The emergence of separation signals could be from the charge carried away by material transfer as a result of bond breaking or bond formation. XPS analysis from few research groups [7, 12, 67] have shown that material transfer occurs between contact materials, and while separating from each other there is possibility of carrying away charges. XPS spectrum of pure PDMS shows C1s (42.9%), Si2p (28.9%) and O1s (28.2%) elemental peaks are shown in Figure 3.9a. We checked possibility of material transfer from PDMS to Al surface by XPS measurement. To do this, PDMS was contacted once with Al surface and separated. Material transfer from polymer to metal is evident from the presence of Si (and O) on the metal surface as shown in Figure 3.9b. This result reveals that breaking of Si-O and Si-C bonds in a 3D networking polymer PDMS takes place and transfer of polymeric material onto Al surface occur.

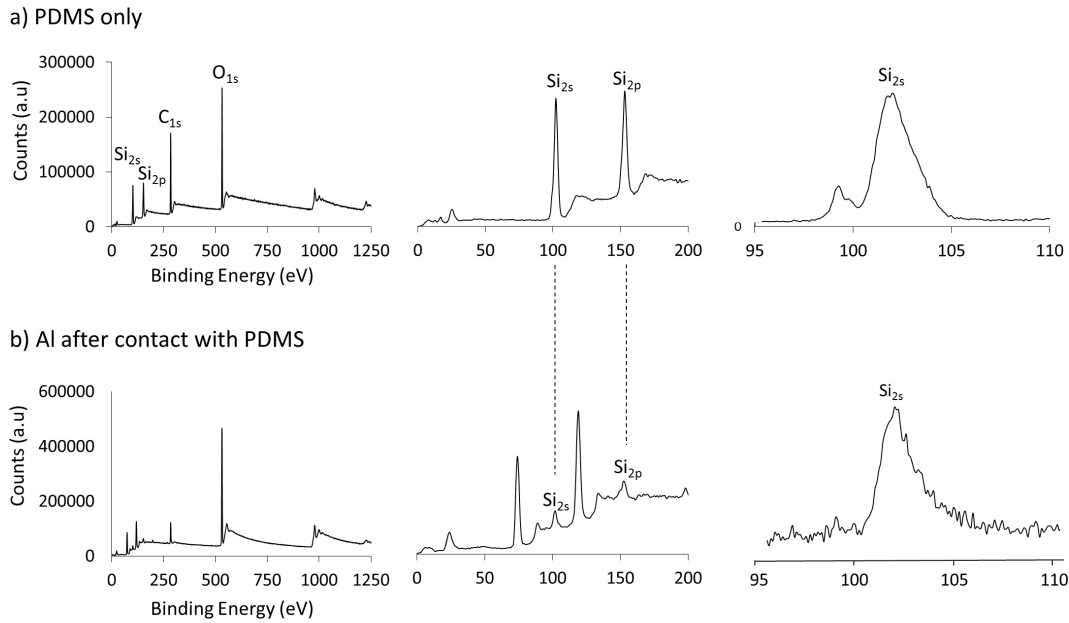


Figure 3.9: XPS surface analysis of pure PDMS and Al after single contact and separation. a) PDMS has C, Si and O atoms, b) Al surface indicates Silicon peaks due to the material transfer from the polymer

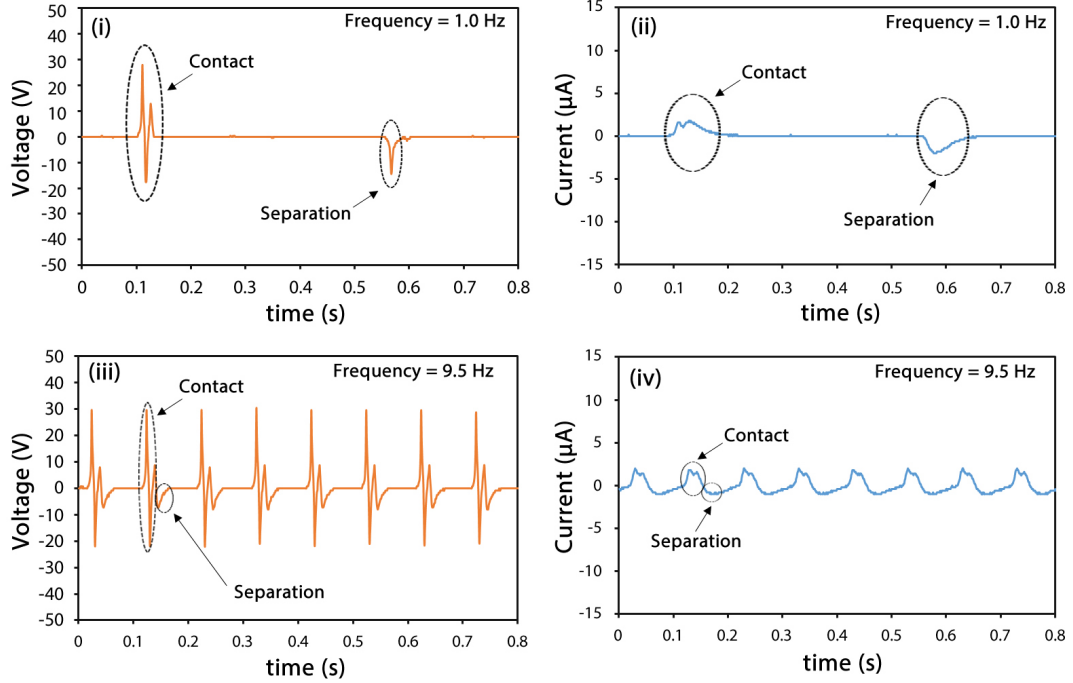
In order to have more perception of contact electrification in relation with change of material thickness we conducted a study by changing the thickness of PDMS. We realised that inductive charge increases with increase in thickness of material and frequency, until a certain point is reached where the open circuit voltage begin to decrease. Figure 3.10 shows some experimental results taken from contact between Cu metal and PDMS of thickness 0.15, 0.24, 0.41 and 0.55 mm.

The graphs in Figure 3.10 indicate how, with increase in frequency from 1 Hz to 9.5 Hz, separation peak nearly disappears or moves very close to the contact peaks. The figure also shows how inductive charge increases with increase in thickness and frequency. With 0.15 mm PDMS at 1.0 Hz a peak-peak voltage of 45.6 V was recorded from contact peaks and 14.4 V from separation, current of 1.8 μA was recorded each from both contact and separation signals. After increasing the frequency to 9.5 Hz at same thickness of 0.15 mm a voltage of 52.0 V was obtained from contact and 8.0 V from the separation, current of 2.0 μA was recorded from contact signals and 1.0 μA from the separation (Figure 3.10a).

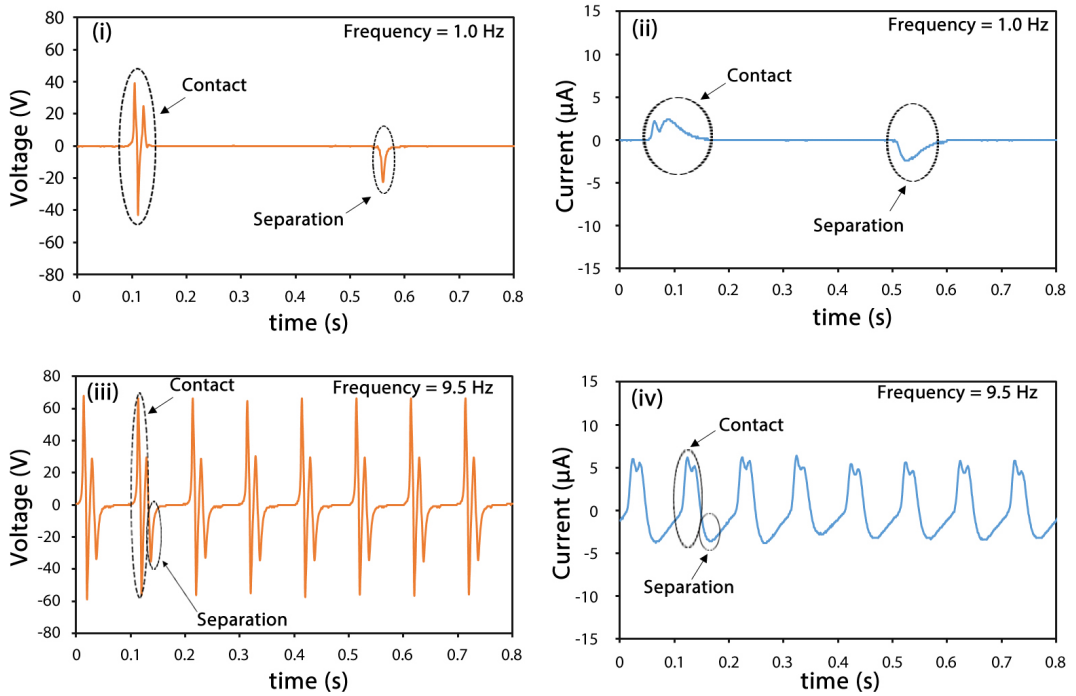
After increasing the thickness of PDMS to 0.24 mm, at 1.0 Hz a voltage of 81.6 V was recorded from contact and 21.6 V from separation, current of 2.4 μA was measured from both contact and separation. After the frequency is increased to 9.5 Hz, 125.6 V was obtained from contact and 26.0 V from separation, current of 5.6 μA was recorded from contact and 2.8 μA separation (Figure 3.10b). These results show how output increases with increase in thickness and frequency.

As the thickness is further increased to 0.41 mm (Figure 3.10c), at 1 Hz both the current and voltage from contact and separation increase. When frequency is changed to 9.5 Hz at same thickness the output remains almost the same with an increase in separation peaks. Figure 3.10d shows decrease in inductive charge, contact and separation output after further increasing the thickness to 0.55 mm. This implies that the polymeric material has reached its limit, as stated by Lowell *et al.* “states that are deep inside bulk of an insulator may not have any impact on contact electrification, because they cannot reach electrons from the contacting metal”. However states which lie near the surface, just as the case of thin polymers, can reach out to the metal because electrons have the ability to tunnel into the polymers around short distances [72].

a) Thickness of PDMS = 0.15 mm



b) Thickness of PDMS = 0.24 mm



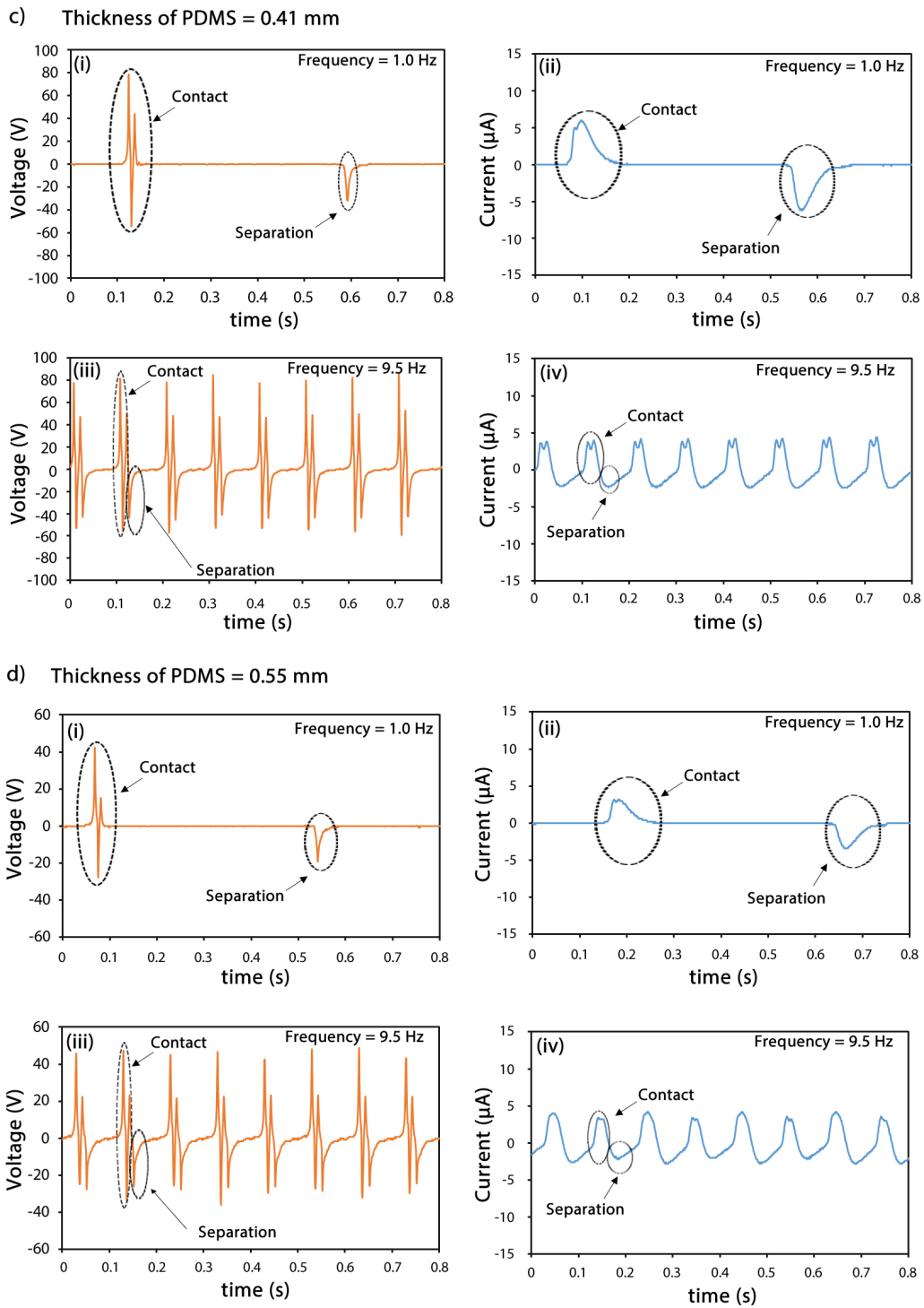


Figure 3.10: Short circuit current and open circuit voltage obtained from thickness test of PDMS in contact with Cu metal at 1.0 and 10.0 Hz, respectively. Results from contact between Cu metal and PDMS of thickness: (a) 0.15 mm, (b) 0.24 mm, (c) 0.41 mm, and (d) 0.55 mm.

To investigate environmental effects on contact electrification some output power test related to humidity and power density dependence on thickness study was conducted. Figure 3.11 illustrates that output performance increases as the thickness increases until 0.41 mm is reached where it begins to decrease. This shows that material thickness has its on limit for obtaining maximum output voltage, current and power density. Humidity test also reveals that the higher the humidity the lower the output power. This probably occurs as a result of moisture in the air which lowers the resistance of material surface by allowing wet conductive water layer over the surface to cause redistribution of charge on the surface.

The output power “P” was calculated from the output voltage “V” and short circuit current “I” measured during contact electrification between 6 mm Cu metal and PDMS of four different thicknesses using the following formular;

$$P = IV \quad (Watt), \quad (3.1)$$

$$Power \ density = \frac{P}{contact \ area} \quad (Watt/m^2) \quad (3.2)$$

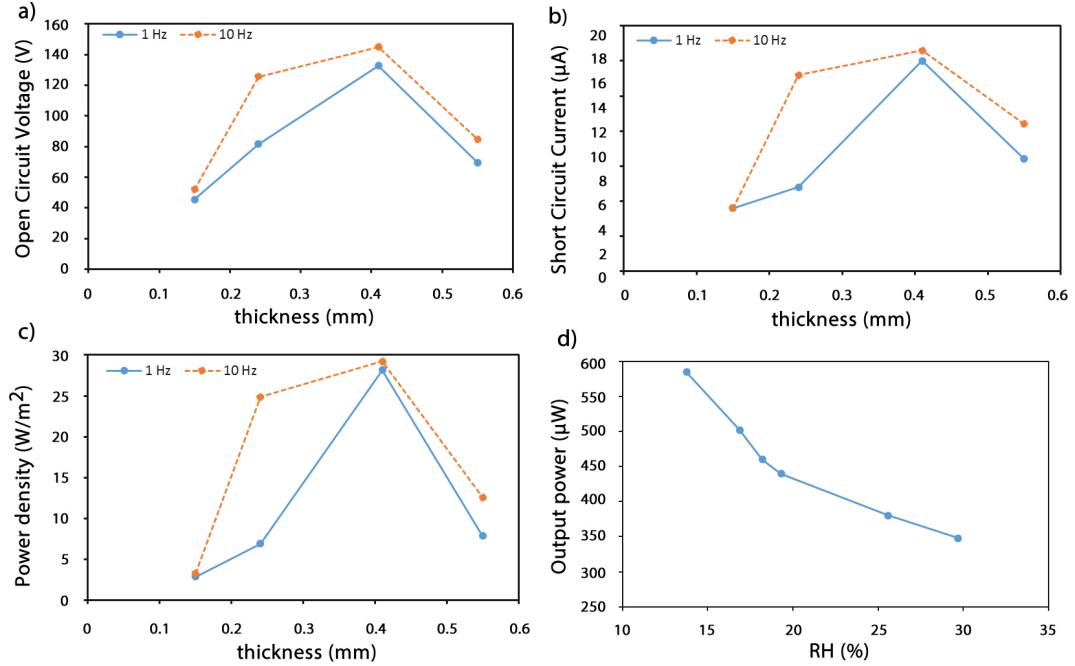


Figure 3.11: Open-circuit voltage, short circuit current and power density dependence on thickness, and output power versus relative humidity relations. a-b) Open-circuit voltage and short circuit current acquired from contact-separation at two different frequencies, 1 and 10 Hz respectively. c) Different power densities obtained from metal-PDMS interaction at 0.28 cm^2 contact surface area with respect to change in frequency. d) humidity dependence of output power generation procured from 6 different measurements at 5 Hz.

3.4 Mechanism of contact electrification

Contact charging results in electric potential difference whenever two materials come in contact and separated [79]. Even though triboelectric effect has been known and applied in technology for so long, the fundamental mechanism is still not well understood [67–80]. Based on experimental evidence we designed and explained our mechanism in detail.

We earlier discussed (in chapter 2) the three basic mechanisms in which charge is transferred from one body to another during contact. Charge transfer is usually due to electron transfer in metal-polymer or polymer-polymer contact [72].

Although, other transfer mechanisms may play vital role in exceptional cases like the contact involving insulators with mobile ions [78]. In this section, we discuss our proposed mechanism in detail by using three kinds of contact tapping frequency; low frequency (1 Hz), moderate frequency (5-10 Hz), and high frequency (>10 Hz).

3.4.1 Mechanism of metal-polymer tribocharging

After careful study of contact electrification using experimental analysis, here we explain our proposed mechanism using three different classifications: low, moderate and high frequency contact and separation based on metal-polymer triboelectrification.

3.4.1.1 Low and moderate frequency contact

The kind of mechanism designed here occurs for contact electrification at low and moderate frequencies only. Figure 3.12 illustrates the proposed mechanism based on metal-polymer (or insulator) contact and separation. Before the contact, materials are at their uncharged state. Positive and negative triboelectric charges are generated on the surface of the polymer as soon as the materials (polymer and metal electrode) touch each other (Figure 3.12d). This charge accumulation is contrary to what many experimentalists think, as explained in the previous chapter (triboelectric series), that every material carries either positive or negative charge alone. However, Baytekin and co-workers [12] used modern characterization techniques to show how both positive and negative charges appear on the surface of either polymers after contact. Negative charges flow from metal electrode (ME) to ground and from ground to base electrode (BE) simultaneously by contact charging; that is, the negative charge produced on the surface of the polymer is directly transferred to ME which then flows to ground, thereby leaving positive charge on the surface of the polymer alone, and attracting electrons from the ground to BE (Figure 3.12e,f). As the polymer retains its positive

surface charge, BE also retains the incoming ground electrons and no charge flow occurs for a while, as shown in Figure 3.12**b** (5) and **g**. There is also back flow of electrons from ground to ME, probably due to tunneling of electron around the interface between contact materials [72]. The back flow occurs simultaneously together with negative charge compensation from BE to ground (Figure 3.12**h,i**). Positive and negative charges are regenerated at the interface of the contact materials while they begin to separate from each other, which gives rise to simultaneous flow of charge; from ME to ground and from ground to BE (Figure 3.12**l,m**). This charge might be as a result of material transferred by bond breaking and formation, which takes away some charges during contact (see material transfer in chapter 2). Then, negative charges remain on base electrode and surface of the polymer, while positive charge remains on the metal electrode. After a complete cycle (contact and separation), charges still remain on the surfaces of both materials and base electrode which gradually decay into air after some time (it could be minutes, hours or days), unless if BE and ME are connected to ground where discharge occurs and the system goes back to Figure 3.12**a** or **c**.

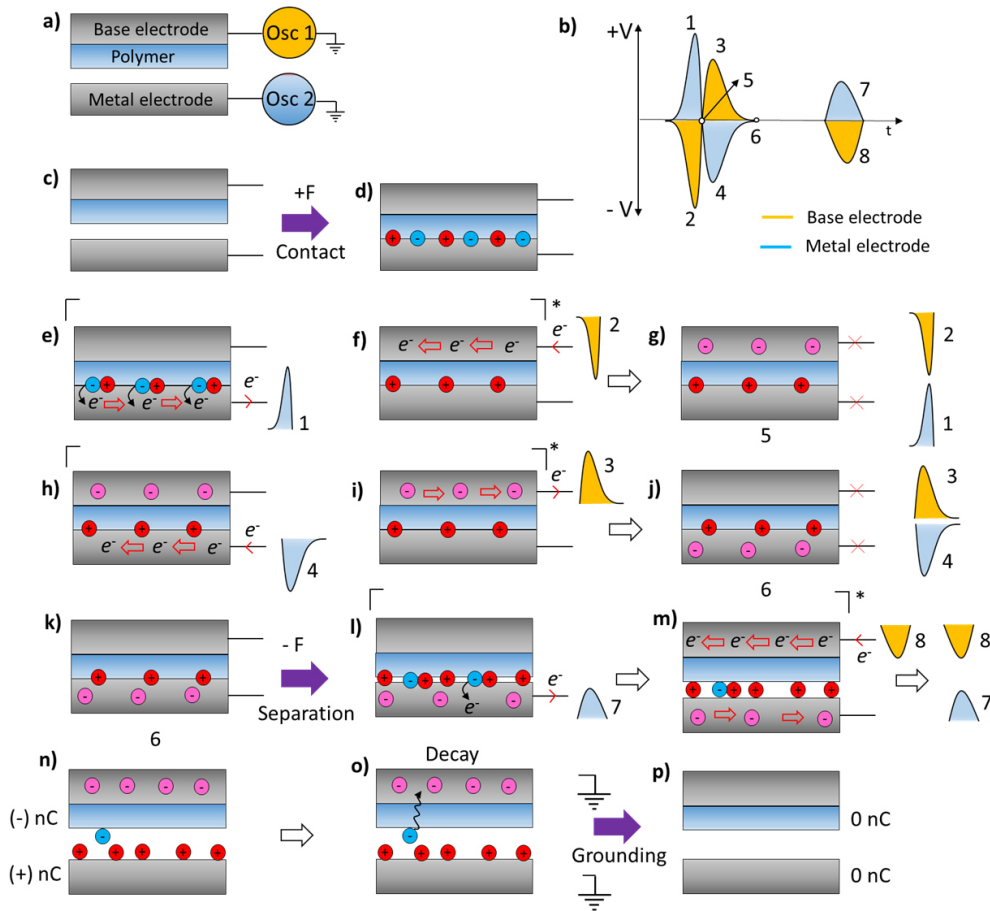


Figure 3.12: Proposed mechanism of contact electrification based on metal-polymer interaction. (a) Before contact the polymer is at uncharged state. (b) Shows the kind of signals obtained (from b to m) in the whole process. (c) Force is applied, metal electrode approaching polymer (which is static on base electrode). (d) Contact and charge generation; positive and negative triboelectric charges are generated on the surface of polymer. (e) Negative charge flow from the surface of polymer to metal electrode (ME) and (f) negative charge flow from ground to the base electrode (BE) occur simultaneously by contact electrification. (g) Polymer retains its positive surface charge, BE retains the incoming negative electrons, and no additional charge flow at this stage. (h) Back flow of charge from ground to ME and (i) negative charge from BE to ground occur concurrently. (j) ME retains the incoming negative charge, no any charge flow and (k) separation set to begin. (l) Positive and negative charge regeneration occurs at the interface of the contact materials (polymer and metal electrode) due to separation, which gives rise to charge flow; from ME to ground and (m) ground to BE at the same time. (n) Negative charges remain on BE and polymer surface, while positive remains on the surface of ME. (o) Decay occurs gradually and (p) when the system is connected to ground, no charge remains in the system.

After initial contact and separation: During experiment, we discovered that after first contact, before second and subsequent contact and separation, charge inductance occurs at very short distance before the materials (polymer and metal electrode) touch each other and while they are separating from each other. At this very small gap the system behaves like an air-gap parallel plate capacitor [86,87]. Charge induction normally occurs when charged materials approach each other by generating electric field in between them [72]. In contact between metal and polymer, charge induction occurs because the remaining charges on both materials after first contact are being transferred. Figure 3.13a depicts how the signals appear with induction peaks for both contact and separation immediately after initial contact and separation at low and moderate frequencies. Charge induction signals appear while the materials are converging (approaching) and diverging (leaving) each other. When force is applied materials start converging each other and no signals appear before initial contact. Signals **C1** appears during the initial contact, and signals **S1** during separation (Figure 3.13a(ii) and (iii)). Convergence induction (I_c) occurs at a very small distance while the materials are converging each other for second contact. The I_c together with the contact give rise to a combination of induction and contact signals **C2** (Figure 3.13a(iv)). As the materials start diverging from each other the separation and divergence induction (I_d) signals **S2** appear, as shown in Figure 3.13a(v)). After the first contact, all subsequent contact and separation give similar results as in **C2** and **S2** which are also similar to **C3** and **S3**. The signals observed are also separated according to oscilloscope channels 1 and 2 in Figure 3.13b,c for clear description of the mechanism.

Figure 3.14 demonstrates the overall signals of metal electrode and polymer obtained at 1 Hz, where the individual channels are plotted separately for clear explanation of the signals obtain at low and moderate frequencies. Figure 3.15 also gives the overall results of the happenings at low, moderate and high frequencies (1, 5, and 10 Hz). The results show how convergence and divergence induction appear after first contact.

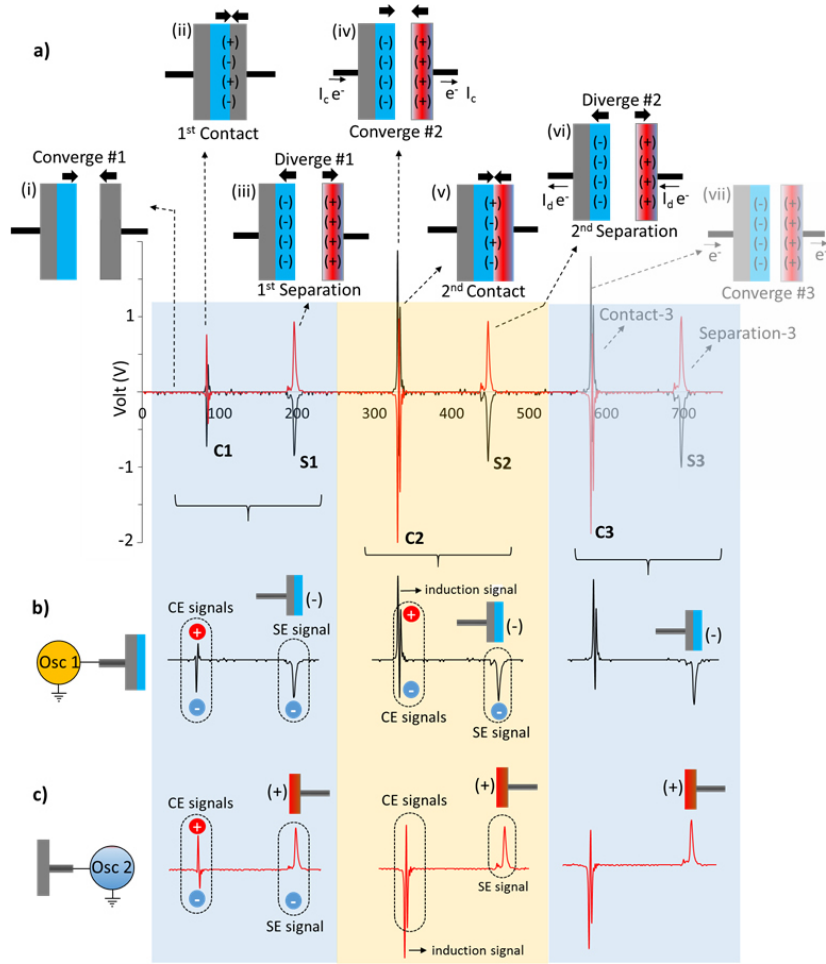


Figure 3.13: Behaviour of the signals **after first contact** based on metal-polymer interaction at low and moderate frequency contacts, where not only separation (SE) and contact (CE) electrification signals are obtained but also charge induction signals appear while the materials are converging and diverging. (a) First, second, and third contact and separation of metal and polymer with their signals: (i) When force is applied materials start approaching each other and no signals obtained. (ii) First contact occurs with contact signals **C1**, and (iii) first separation occurs while the two materials are diverging from each other which produces signals **S1**. (iv) Charge induction (I_c) occurs at a very small gap while the materials are about to touch each other, and (v) second contact occurs immediately, giving rise to a combination of induction and contact signals **C2**. (vi) Second separation occurs while the materials are separating, thereby generating separation and divergence charge induction (I_d) signals **S2**. (vii) Third contact and separation gives similar signals **C3** and **S3** with second contact, which is same for every contact/separation after the initial contact and separation. Signals observed from oscilloscope channels 1 and 2: (b) Oscilloscope channel 1, connected to BE and polymer, shows all the signals obtained in (a) via channel 1. (c) Oscilloscope channel 2, connected to ME, indicates all the signals obtained through the second channel.

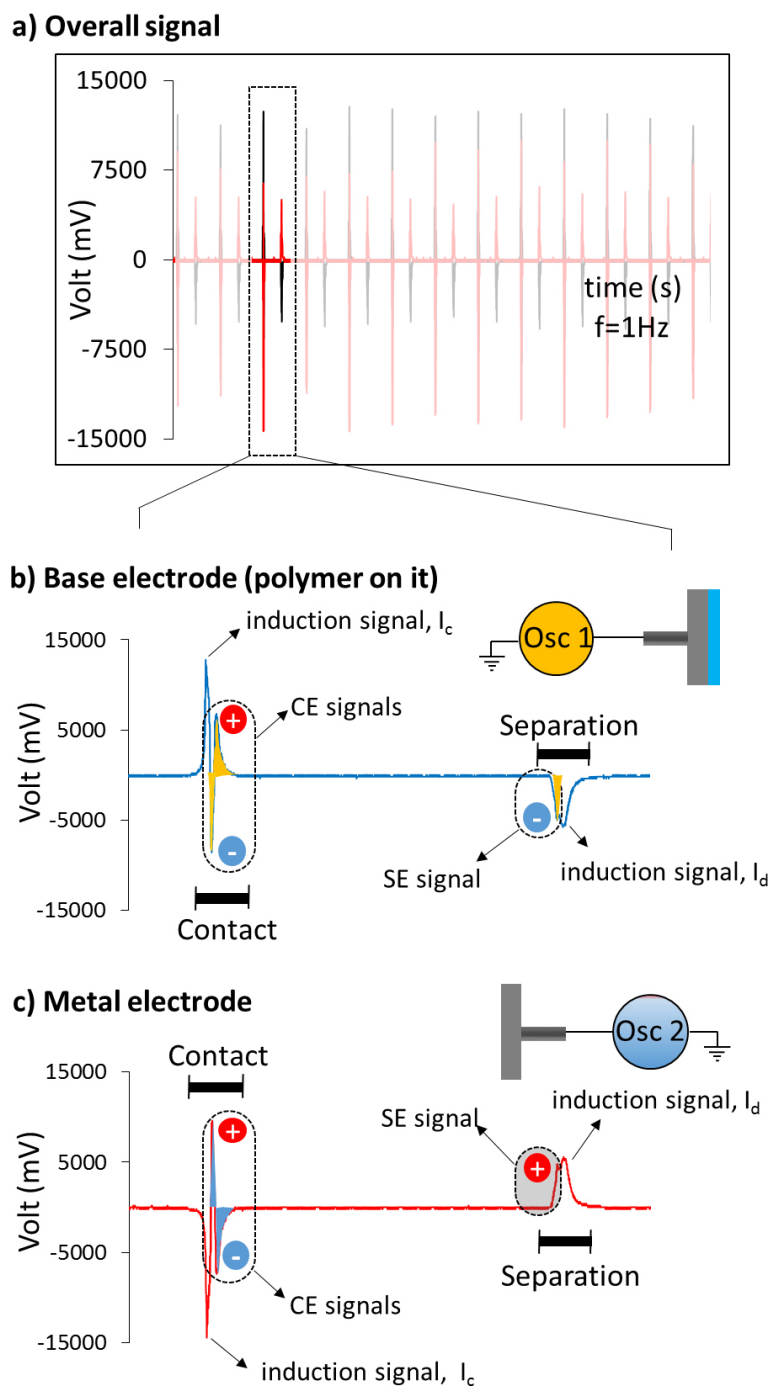


Figure 3.14: Overall outcome of metal-polymer contacts with their respective channel signals. (a) Overall signal for for subsequent contacts at 1 Hz. (b) signals recorded from base electrode (channel 1). (C) signals obtained from metal electrode (channel 2).

3.4.1.2 High frequency contact

We discovered that at high frequencies (>10 Hz) the observed signals appear as a combination of two peaks; a single peak from contact and a single peak with opposite polarity from separation. The results in Figure 3.15g,h have clearly shown the occurrences at high frequencies, where convergence induction, divergence induction, contact and separation signals merge together due to high tapping frequency ($I_c+CE+SE+I_d$). Prior to contact, materials are at uncharged state. Thus, at high frequency I_c and CE combine to form a single peak (appeared as positive signal in Figure 3.15g), while SE and I_d combine to form a single peak of opposite polarity (appeared as negative signal in Figure 3.15f). This is the reason why contact electrification cannot be regarded as a process that gives rise to **only** positive peak during contact and a negative peak during separation. Thus, we have clearly shown how people unknowingly concluded that contact and separation between two materials gives only two peaks (positive and negative).

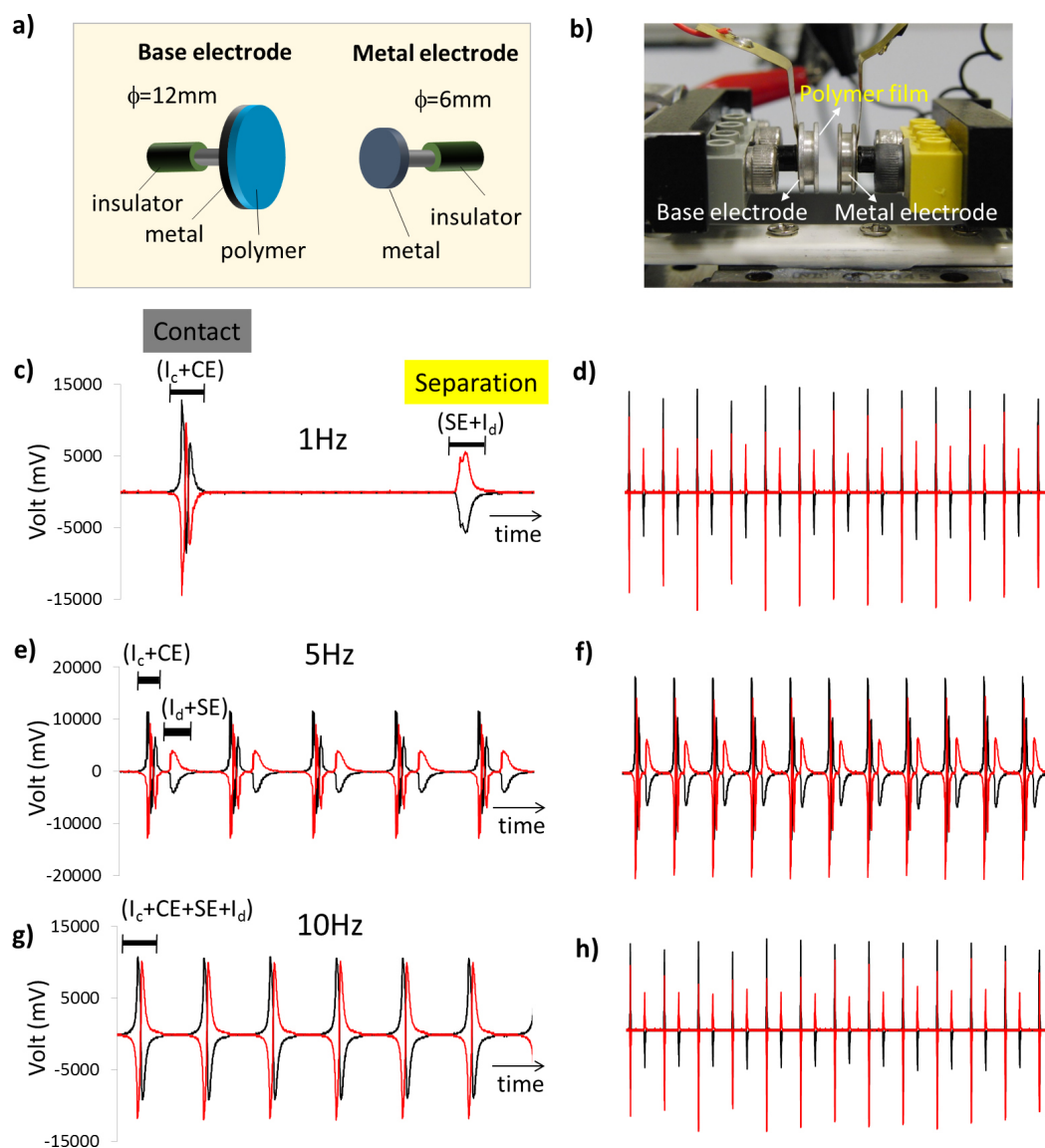


Figure 3.15: (a) Design of contact base electrode with a polymer of diameter 12 mm and Cu metal electrode of 6 mm diameter. (b) Picture showing BE with polymer thin film and ME. (c,d) Results showing three peaks from combined CE and I_c signals and separation signals (SE and I_d) at 1 Hz. (e,f) Shows I_c and CE combined, while separation signals move closer to contact as a combination of I_d and SE at 5 Hz. (g,h) Now all the signals appear as a single signal of two peaks ($I_c + CE + SE + I_d$). This is the common signal in the published results which cause a big confusion in assigning the contact-separation electric signals. (PP was the polymer used to show the general behaviour of contact and separation peaks at low, moderate and high frequencies for all kind of polymers).

3.4.1.3 Evidence of electron transfer from polymer to metal

We used light emitting diode (LED) in forward and reverse connections to verify our proposed triboelectrification mechanism. The forward polarity of the LED is a way of connecting the Anode (+) of the LED to metal electrode and the Cathode (−) to ground, while the reverse polarity is a way of connecting Cathode to the metal electrode and Anode to the ground.

We tested the LED using contact and separation between PTFE and Cu metal. Based on our mechanism, we connected the Cathode (−) of the LED to the metal electrode (reverse polarity) and observed light as the polymer touched the metal surface (Figure 3.16a (i)). When the metal electrode is connected to the Anode (+) of the LED (forward polarity) no light was observed, as shown in Figure 3.16a (ii). However, according to a large number of published results in the literature and [60], [72] electron transfer from metal to polymer is regarded as the only possibility of charge transfer between the metal-polymer, transfer from polymer to metal is accepted as impossible. Also, after separation light was observed from forward polarity which verifies transfer of electrons from polymer to metal during contact (Figure 3.16b (i)), and no light was observed after separation in the reverse polarity which indicates that no transfer of electron from metal to polymer.

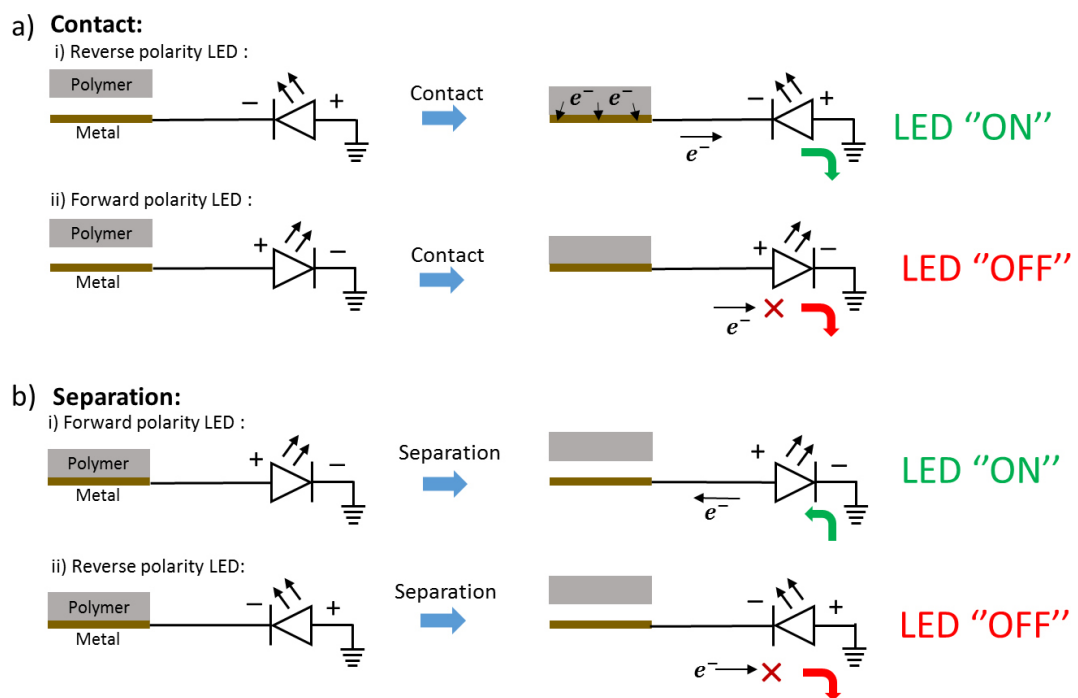


Figure 3.16: Electron transfer from polymer to metal contact electrification with LED connected: (a) During contact in (i) reverse polarity and (ii) forward polarity of the LED. (b) After separation in (i) reverse polarity and (ii) forward polarity of the LED

3.4.2 Mechanism of polymer-polymer tribocharging

Metal-metal and metal-polymer triboelectrification are now theoretically better understood phenomena, whereas polymer-polymer contact charging is the least recognized triboelectric phenomenon. Some researchers have stated that ion exchange is probably the mechanism of contact electrification between two insulators, because they do not contain mobile electrons in their conduction bands [88]. As mentioned in the previous chapter some diverse models, which are congruent with metal-polymer contact, were presented in order to make electron transfer possible in polymer-polymer contact [71, 72].

Based on experimental evidence, we realized that polymer-polymer contact charging **has exactly the same mechanism** as that of the metal-polymer contact explained in the previous section. The process is not redrawn here because it repeatedly gives very similar results to that of metal-polymer interactions seen in the results and discussions section.

Pure PDMS and AuNp-PDMS composites were used for polymer-polymer contact electrification experiment. The experiments show that doping PDMS with AuNp is another way of controlling its triboelectric charge. The samples used are shown in Figure 3.17a which comprises of 0, 0.5, 0.99, 1.96 and 3.85 % of Au in 1 gram of PDMS each. SEM images of the pure PDMS and AuNp doped PDMS (taken at 10.0 KV, spot size of 3.0 and 100 microns) are shown in Figure 3.17b,c.

The graphs in Figure 3.18 show the signals observed from contact electrification experiments between ME and PDMS-AuNp composites, two pure PDMS, and pure PDMS with AuNp doped PDMS samples which contain 0.5, 0.99, 1.96 and 3.85 % of Au in 1 gram of PDMS each. We realised that contact and separation between metal and pure PDMS always gives the maximum output voltage, followed by the pure PDMS-pure PDMS contact. We obtained maximum and minimum output voltages of approximately 36.8 and 2.2 volts from contact between pure PDMS with Al metal and AuNp-PDMS composite containing 3.85 % of Au in 1 gram of PDMS. From our results we realised that the lower the

percentage of the gold nanoparticles in the composite the better the output voltage becomes, as shown in Figure 3.18**b-f**. The average open-circuit voltage per gold percentage in 1 gram of PDMS (1/201, 1/101, 1/51, and 1/25 AuNp-PDMS weight ratios) are shown in Figure 3.18**g,h**.

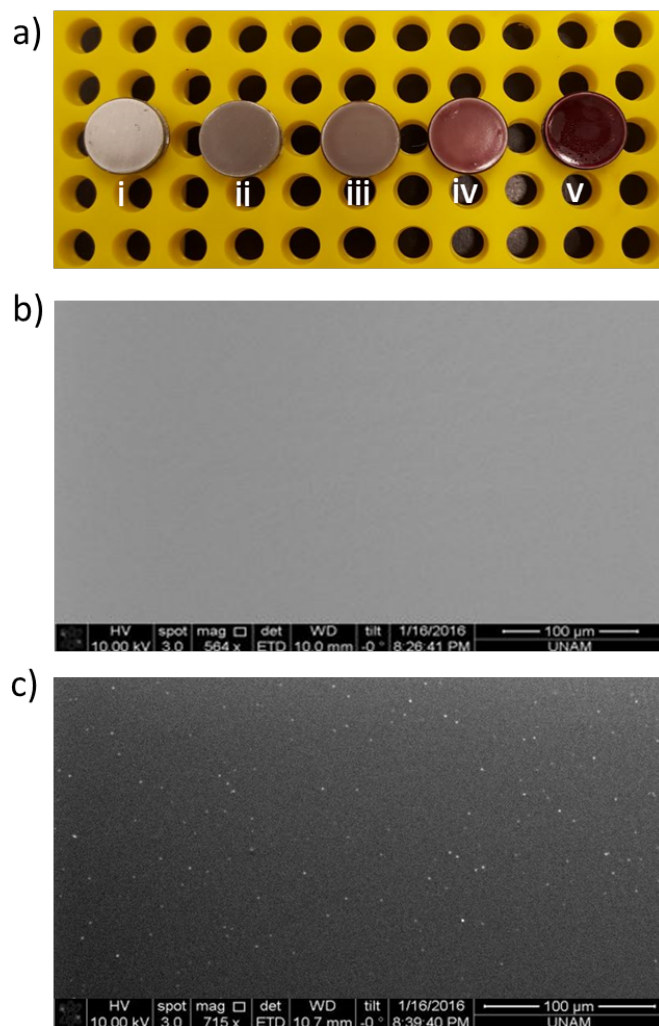


Figure 3.17: (a) Samples used. From left to right; (i) Pure PDMS, AuNp-PDMS composites (ii) 0.5, (iii) 0.99, (iv) 1.96 and (v) 3.85 % of Au in 1 gram of PDMS each. (b) SEM images of pure PDMS at magnification of 564 x, and (c) Au doped PDMS (5 mg Au in 1 gram of PDMS = 1.96 %) with 539 x magnification and the percentages of gold in 1 gram of PDMS.

We think that there are two possibilities for the decrease in output voltage as the amount of gold percent is increased in PDMS: (1) There is possibility of charge trapping, because in theory the output is expected to be: P-M > P-P(d) > P-P and we experimentally observed: P-M > P-P > P-P(d). This could be as a result of charge trapping caused by the increase in gold nanoparticle in the polymer metal composites. (2) There is possibility of change in material property, e.g. elasticity. (P = pure PDMS, M = metal, and P(d) = doped PDMS).

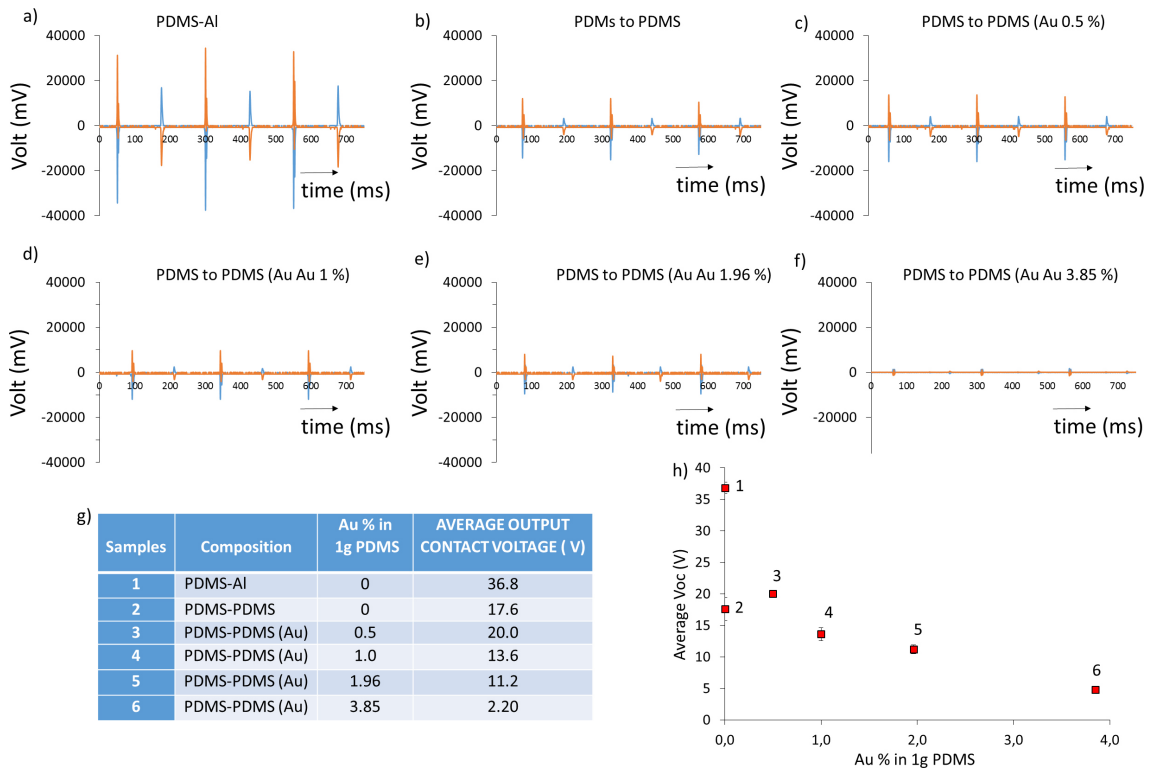


Figure 3.18: Signals obtained by doping pure PDMS samples with Au of 0, 0.5, 1.0, 1.96, and 3.85 Au% in 1 gram of PDMS with their average output voltages.

Chapter 4

Conclusion

In this study, contact electrification of metal-polymer and polymer-polymer were rigorously analysed. Controversy over the mechanism(s) of contact electrification between dielectric materials and metal-dielectric has led us to develop a reliable triboelectric charge generating device for testing all kinds of polymers to enable a thorough study of the fundamentals of triboelectricity at any kind of frequency. While trying to deeply digest the issue, we discover and propose a mechanism which is very crucial towards understanding some unanswered questions on triboelectrification.

Materials were systematically tested at low, moderate, and high frequencies for thorough investigation of the basics of static electricity. Based on experimental outcomes, we realised that for decades triboelectrification has been misunderstood due to negligence or lack of careful investigation. Our results have shown a clear contradiction to what we read every day from the literature, that two charges of opposite polarities are produced whenever two materials are brought into contact and separated. That is, the results we obtained from contact charging of two materials (be it metal-dielectric or dielectric-dielectric) have shown contradiction to what most of the researchers working in the field believe to be the mechanism(s) of contact electrification.

The Literature results have indicated that researchers usually care about generating high electrical output alone, while neglecting the knowledge of how the triboelectric effect generates electricity, and so forth. In an attempt to find answers to some controversial issues, we used our own mechanical tapping device to observe the triboelectric charge of polymers at different frequencies. After carefully studying the contact electrification between two materials (identical or dissimilar), we discover and propose a new mechanism which is contrary to the all available mechanisms in the literature. Our mechanism indicates a combination of both positive and negative charges during contact and a single separation peak (either positive or negative) during separation, both of which generate charge induction in subsequent contact and separation, immediately after the first contact-separation.

We have also realised that charge generation is not equal to charge transfer, as it is generally assumed to be. We showed that charges are generated on the surface of material in charge generation, while charge transfer occurs only when the charges are already there. We have clearly shown the difference between them in our proposed contact electrification mechanism. Obviously, the concept of triboelectrification is generally misconceived either by not giving careful attention to it or by failing to understand the real effect. We are certain that our newly proposed mechanism of tribocharging will play vital role towards apprehending some pending issues on contact electrification, like the uncertain separation peaks usually observed from touch sensors and other energy harvesting devices that operate at low and moderate frequencies, and so on.

Bibliography

- [1] R. G. Horn and D. T. Smith, “Contact electrification and adhesion between dissimilar materials,” *Science*, vol. 256, no. 5055, p. 362, 1992.
- [2] R. G. Horn, D. Smith, and A. Grabbe, “Contact electrification induced by monolayer modification of a surface and relation to acid-base interactions,” *Nature*, vol. 366, pp. 442–443, 1993.
- [3] K. Nakayama, “Tribocharging and friction in insulators in ambient air,” *Wear*, vol. 194, no. 1, pp. 185–189, 1996.
- [4] T. A. Burgo, C. A. Silva, L. B. Balestrin, and F. Galembeck, “Friction coefficient dependence on electrostatic tribocharging,” *Scientific reports*, vol. 3, 2013.
- [5] D. J. Lacks and R. M. Sankaran, “Contact electrification of insulating materials,” *Journal of Physics D: Applied Physics*, vol. 44, no. 45, p. 453001, 2011.
- [6] S. Soh, H. Liu, R. Cademartiri, H. J. Yoon, and G. M. Whitesides, “Charging of multiple interacting particles by contact electrification,” *Journal of the American Chemical Society*, vol. 136, no. 38, pp. 13348–13354, 2014.
- [7] M. W. Williams, “Triboelectric charging of insulating polymers—some new perspectives,” *AIP Advances*, vol. 2, no. 1, p. 010701, 2012.
- [8] T. Mather and R. Harrison, “Electrification of volcanic plumes,” *Surveys in Geophysics*, vol. 27, no. 4, pp. 387–432, 2006.

- [9] T. Miura, T. Koyaguchi, and Y. Tanaka, “Measurements of electric charge distribution in volcanic plumes at sakurajima volcano, japan,” *Bulletin of volcanology*, vol. 64, no. 2, pp. 75–93, 2002.
- [10] F. Galembeck, T. A. Burgo, L. B. Balestrin, R. F. Gouveia, C. A. Silva, and A. Galembeck, “Friction, tribochemistry and triboelectricity: recent progress and perspectives,” *RSC Advances*, vol. 4, no. 109, pp. 64280–64298, 2014.
- [11] J. A. Wiles, B. A. Grzybowski, A. Winkleman, and G. M. Whitesides, “A tool for studying contact electrification in systems comprising metals and insulating polymers,” *Analytical chemistry*, vol. 75, no. 18, pp. 4859–4867, 2003.
- [12] H. Baytekin, A. Patashinski, M. Branicki, B. Baytekin, S. Soh, and B. A. Grzybowski, “The mosaic of surface charge in contact electrification,” *Science*, vol. 333, no. 6040, pp. 308–312, 2011.
- [13] X.-J. Zheng, “Electrification of wind-blown sand: Recent advances and key issues,” *The European Physical Journal E*, vol. 36, no. 12, pp. 1–15, 2013.
- [14] K. M. Forward, *Triboelectrification of granular materials*. PhD thesis, Case Western Reserve University, 2009.
- [15] S. Matsusaka, H. Maruyama, T. Matsuyama, and M. Ghadiri, “Triboelectric charging of powders: A review,” *Chemical Engineering Science*, vol. 65, no. 22, pp. 5781–5807, 2010.
- [16] A. G. Bailey, “The charging of insulator surfaces,” *Journal of Electrostatics*, vol. 51, pp. 82–90, 2001.
- [17] P. Iversen and D. J. Lacks, “A life of its own: The tenuous connection between thales of miletus and the study of electrostatic charging,” *Journal of Electrostatics*, vol. 70, no. 3, pp. 309–311, 2012.
- [18] W. R. Smythe, *Static and dynamic electricity*. Hemisphere Publishing Corporation New York, 3 ed., 1989.

- [19] R. P. Olenick, T. M. Apostol, and D. L. Goodstein, *Beyond the mechanical universe: from electricity to modern physics*. Cambridge University Press, 1986.
- [20] W. F. Magie *et al.*, “Source book in physics,” pp. 387–402, 1969.
- [21] D. A. Seanor, *Electrical properties of polymers*. Elsevier, 2013.
- [22] M. Lungu, “Electrical separation of plastic materials using the triboelectric effect,” *Minerals Engineering*, vol. 17, no. 1, pp. 69–75, 2004.
- [23] G. Castle, “Contact charging between insulators,” *Journal of Electrostatics*, vol. 40, pp. 13–20, 1997.
- [24] L. B. Loeb, “The basic mechanisms of static electrification,” *Science*, vol. 102, no. 2658, pp. 573–576, 1945.
- [25] H. Mizes, E. Conwell, and D. Salamida, “Direct observation of ion transfer in contact charging between a metal and a polymer,” *Applied physics letters*, vol. 56, no. 16, pp. 1597–1599, 1990.
- [26] H. T. Baytekin, B. Baytekin, S. Soh, and B. A. Grzybowski, “Is water necessary for contact electrification?,” *Angewandte Chemie International Edition*, vol. 50, no. 30, pp. 6766–6770, 2011.
- [27] Z.-H. Lin, Y. Xie, Y. Yang, S. Wang, G. Zhu, and Z. L. Wang, “Enhanced triboelectric nanogenerators and triboelectric nanosensor using chemically modified tio2 nanomaterials,” *ACS nano*, vol. 7, no. 5, pp. 4554–4560, 2013.
- [28] M. Kanik, M. G. Say, B. Daglar, A. F. Yavuz, M. H. Dolas, M. M. El-Ashry, and M. Bayindir, “A motion-and sound-activated, 3d-printed, chalcogenide-based triboelectric nanogenerator,” *Advanced Materials*, vol. 27, no. 14, pp. 2367–2376, 2015.
- [29] S. Wang, L. Lin, and Z. L. Wang, “Nanoscale triboelectric-effect-enabled energy conversion for sustainably powering portable electronics,” *Nano letters*, vol. 12, no. 12, pp. 6339–6346, 2012.

- [30] Z.-H. Lin, G. Cheng, Y. Yang, Y. S. Zhou, S. Lee, and Z. L. Wang, "Triboelectric nanogenerator as an active uv photodetector," *Advanced Functional Materials*, vol. 24, no. 19, pp. 2810–2816, 2014.
- [31] J. Yang, J. Chen, Y. Yang, H. Zhang, W. Yang, P. Bai, Y. Su, and Z. L. Wang, "Broadband vibrational energy harvesting based on a triboelectric nanogenerator," *Advanced Energy Materials*, vol. 4, no. 6, 2014.
- [32] Z. L. Wang, "Nanogenerators for self-powered devices and systems," 2011.
- [33] Y. Su, J. Chen, Z. Wu, and Y. Jiang, "Low temperature dependence of triboelectric effect for energy harvesting and self-powered active sensing," *Applied Physics Letters*, vol. 106, no. 1, p. 013114, 2015.
- [34] G. Zhu, J. Chen, Y. Liu, P. Bai, Y. S. Zhou, Q. Jing, C. Pan, and Z. L. Wang, "Linear-grating triboelectric generator based on sliding electrification," *Nano letters*, vol. 13, no. 5, pp. 2282–2289, 2013.
- [35] Y. K. Pang, X. H. Li, M. X. Chen, C. B. Han, C. Zhang, and Z. L. Wang, "Triboelectric nanogenerators as a self-powered 3d acceleration sensor," *ACS applied materials & interfaces*, vol. 7, no. 34, pp. 19076–19082, 2015.
- [36] H. Zhang, Y. Yang, X. Zhong, Y. Su, Y. Zhou, C. Hu, and Z. L. Wang, "Single-electrode-based rotating triboelectric nanogenerator for harvesting energy from tires," *Acs Nano*, vol. 8, no. 1, pp. 680–689, 2013.
- [37] K. Y. Lee, J. Chun, J.-H. Lee, K. N. Kim, N.-R. Kang, J.-Y. Kim, M. H. Kim, K.-S. Shin, M. K. Gupta, J. M. Baik, *et al.*, "Hydrophobic sponge structure-based triboelectric nanogenerator," *Advanced Materials*, vol. 26, no. 29, pp. 5037–5042, 2014.
- [38] F. R. Fan, J. Luo, W. Tang, C. Li, C. Zhang, Z. Tian, and Z. L. Wang, "Highly transparent and flexible triboelectric nanogenerators: performance improvements and fundamental mechanisms," *Journal of Materials Chemistry A*, vol. 2, no. 33, pp. 13219–13225, 2014.
- [39] Y. Yang, H. Zhang, J. Chen, Q. Jing, Y. S. Zhou, X. Wen, and Z. L. Wang, "Single-electrode-based sliding triboelectric nanogenerator for self-powered

- displacement vector sensor system,” *Acs Nano*, vol. 7, no. 8, pp. 7342–7351, 2013.
- [40] H. Zhang, Y. Yang, Y. Su, J. Chen, K. Adams, S. Lee, C. Hu, and Z. L. Wang, “Triboelectric nanogenerator for harvesting vibration energy in full space and as self-powered acceleration sensor,” *Advanced Functional Materials*, vol. 24, no. 10, pp. 1401–1407, 2014.
- [41] S. Niu, S. Wang, L. Lin, Y. Liu, Y. S. Zhou, Y. Hu, and Z. L. Wang, “Theoretical study of contact-mode triboelectric nanogenerators as an effective power source,” *Energy & Environmental Science*, vol. 6, no. 12, pp. 3576–3583, 2013.
- [42] G. Castle, “Industrial applications of electrostatics:: the past, present and future,” *Journal of Electrostatics*, vol. 51, pp. 1–7, 2001.
- [43] D. J. Lacks and A. Levandovsky, “Effect of particle size distribution on the polarity of triboelectric charging in granular insulator systems,” *Journal of Electrostatics*, vol. 65, no. 2, pp. 107–112, 2007.
- [44] H. Watanabe, M. Ghadiri, T. Matsuyama, Y. L. Ding, K. G. Pitt, H. Maruyama, S. Matsusaka, and H. Masuda, “Triboelectrification of pharmaceutical powders by particle impact,” *International journal of pharmaceuticals*, vol. 334, no. 1, pp. 149–155, 2007.
- [45] P. Bai, G. Zhu, Y. S. Zhou, S. Wang, J. Ma, G. Zhang, and Z. L. Wang, “Dipole-moment-induced effect on contact electrification for triboelectric nanogenerators,” *Nano Research*, vol. 7, no. 7, pp. 990–997, 2014.
- [46] D. A. Seanor, “Triboelectrification of polymers-a chemist’s viewpoint,” in *Physicochemical aspects of polymer surfaces*, pp. 477–506, Springer, 1983.
- [47] D. J. Lacks and R. M. Sankaran, “Triboelectric charging in single-component particle systems,” *Particulate Science and Technology*, vol. 34, no. 1, pp. 55–62, 2016.
- [48] K. Homewood, “Surface contamination and contact electrification,” in *Treatise on Clean Surface Technology*, pp. 235–245, Springer, 1987.

- [49] R. Mukherjee, V. Gupta, S. Naik, S. Sarkar, V. Sharma, P. Peri, and B. Chaudhuri, “Effects of particle size on the triboelectrification phenomenon in pharmaceutical excipients: experiments and multi-scale modeling,” *Asian Journal of Pharmaceutical Sciences*, 2016.
- [50] P. Holdstock and J. Smallwood, “Measurement of electrostatic discharge ignition risks from conductive components of personal protective equipment,” *Journal of Electrostatics*, vol. 71, no. 3, pp. 509–512, 2013.
- [51] J. Smallwood, “Standardisation of electrostatic test methods and electrostatic discharge prevention measures for the world market,” *Journal of electrostatics*, vol. 63, no. 6, pp. 501–508, 2005.
- [52] T. Zhou, C. Zhang, C. B. Han, F. R. Fan, W. Tang, and Z. L. Wang, “Woven structured triboelectric nanogenerator for wearable devices,” *ACS applied materials & interfaces*, vol. 6, no. 16, pp. 14695–14701, 2014.
- [53] J. Chen, H. Guo, X. He, G. Liu, Y. Xi, H. Shi, and C. Hu, “Enhancing performance of triboelectric nanogenerator by filling high dielectric nanoparticles into sponge pdms film,” *ACS applied materials & interfaces*, vol. 8, no. 1, pp. 736–744, 2015.
- [54] G. Zhu, J. Chen, T. Zhang, Q. Jing, and Z. L. Wang, “Radial-arrayed rotary electrification for high performance triboelectric generator,” *Nature communications*, vol. 5, 2014.
- [55] V. Nguyen, R. Zhu, and R. Yang, “Environmental effects on nanogenerators,” *Nano Energy*, vol. 14, pp. 49–61, 2015.
- [56] K. Zhang, X. Wang, Y. Yang, and Z. L. Wang, “Hybridized electromagnetic–triboelectric nanogenerator for scavenging biomechanical energy for sustainably powering wearable electronics,” *ACS nano*, vol. 9, no. 4, pp. 3521–3529, 2015.
- [57] P. Bai, G. Zhu, Z.-H. Lin, Q. Jing, J. Chen, G. Zhang, J. Ma, and Z. L. Wang, “Integrated multilayered triboelectric nanogenerator for harvesting biomechanical energy from human motions,” *ACS nano*, vol. 7, no. 4, pp. 3713–3719, 2013.

- [58] H. Guo, Z. Wen, Y. Zi, M.-H. Yeh, J. Wang, L. Zhu, C. Hu, and Z. L. Wang, “A water-proof triboelectric–electromagnetic hybrid generator for energy harvesting in harsh environments,” *Advanced Energy Materials*, 2015.
- [59] Z. L. Wang, L. Lin, J. Chen, S. Niu, and Y. Zi, “Harvesting wind energy,” in *Triboelectric Nanogenerators*, pp. 259–282, Springer, 2016.
- [60] Z. L. Wang, L. Lin, J. Chen, S. Niu, and Y. Zi, “Triboelectrification,” in *Triboelectric Nanogenerators*, pp. 1–19, Springer, 2016.
- [61] Z. L. Wang, “Triboelectric nanogenerators as new energy technology for self-powered systems and as active mechanical and chemical sensors,” *ACS nano*, vol. 7, no. 11, pp. 9533–9557, 2013.
- [62] D. J. Lacks, “The unpredictability of electrostatic charging,” *Angewandte Chemie International Edition*, vol. 51, no. 28, pp. 6822–6823, 2012.
- [63] M. W. Williams, “Mechanisms of triboelectric charging of insulators, a coherent scenario,” *Proc. ESA Annual Meeting on Electrostatics 2011*.
- [64] B. Kwetkus, “Particle triboelectrification and its use in the electrostatic separation process,” *Particulate science and technology*, vol. 16, no. 1, pp. 55–68, 1998.
- [65] J. A. Wiles, M. Fialkowski, M. R. Radowski, G. M. Whitesides, and B. A. Grzybowski, “Effects of surface modification and moisture on the rates of charge transfer between metals and organic materials,” *The Journal of Physical Chemistry B*, vol. 108, no. 52, pp. 20296–20302, 2004.
- [66] K. M. Forward, D. J. Lacks, and R. M. Sankaran, “Methodology for studying particle–particle triboelectrification in granular materials,” *Journal of Electrostatics*, vol. 67, no. 2, pp. 178–183, 2009.
- [67] H. T. Baytekin, B. Baytekin, J. T. Incorvati, and B. A. Grzybowski, “Material transfer and polarity reversal in contact charging,” *Angewandte Chemie*, vol. 124, no. 20, pp. 4927–4931, 2012.

- [68] J. J. Cole, C. R. Barry, R. J. Knuesel, X. Wang, and H. O. Jacobs, “Nanocontact electrification: patterned surface charges affecting adhesion, transfer, and printing,” *Langmuir*, vol. 27, no. 11, pp. 7321–7329, 2011.
- [69] Z.-Z. Yu and P. Watson, “Contact charge accumulation and reversal on polystyrene and ptfе films upon repeated contacts with mercury,” *Journal of Physics D: Applied Physics*, vol. 22, no. 6, p. 798, 1989.
- [70] D. M. Gooding and G. K. Kaufman, “Tribocharging and the triboelectric series,” *Encyclopedia of Inorganic and Bioinorganic Chemistry*, 2014.
- [71] L. Lieng-Huang, “Dual mechanism for metal-polymer contact electrification,” *Journal of Electrostatics*, vol. 32, no. 1, pp. 1–29, 1994.
- [72] J. Lowell and A. Rose-Innes, “Contact electrification,” *Advances in Physics*, vol. 29, no. 6, pp. 947–1023, 1980.
- [73] M. Akbulut, A. R. Godfrey Alig, and J. Israelachvili, “Triboelectrification between smooth metal surfaces coated with self-assembled monolayers (sams),” *The Journal of Physical Chemistry B*, vol. 110, no. 44, pp. 22271–22278, 2006.
- [74] W. R. Harper, *Contact and frictional electrification*. Clarendon Press, 1967.
- [75] L. B. Loeb, “The basic mechanisms of static electrification,” *Science*, vol. 102, no. 2658, pp. 573–576, 1945.
- [76] L. S. McCarty and G. M. Whitesides, “Electrostatic charging due to separation of ions at interfaces: contact electrification of ionic electrets,” *Angewandte Chemie International Edition*, vol. 47, no. 12, pp. 2188–2207, 2008.
- [77] W. Salaneck, A. Paton, and D. Clark, “Double mass transfer during polymer-polymer contacts,” *Journal of Applied Physics*, vol. 47, no. 1, pp. 144–147, 1976.
- [78] J. Lowell, “The role of material transfer in contact electrification,” *Journal of Physics D: Applied Physics*, vol. 10, no. 17, p. L233, 1977.

- [79] S. Soh, S. W. Kwok, H. Liu, and G. M. Whitesides, “Contact de-electrification of electrostatically charged polymers,” *Journal of the American Chemical Society*, vol. 134, no. 49, pp. 20151–20159, 2012.
- [80] A. Diaz and R. Felix-Navarro, “A semi-quantitative tribo-electric series for polymeric materials: the influence of chemical structure and properties,” *Journal of Electrostatics*, vol. 62, no. 4, pp. 277–290, 2004.
- [81] Y. Yang, H. Zhang, X. Zhong, F. Yi, R. Yu, Y. Zhang, and Z. L. Wang, “Electret film-enhanced triboelectric nanogenerator matrix for self-powered instantaneous tactile imaging,” *ACS applied materials & interfaces*, vol. 6, no. 5, pp. 3680–3688, 2014.
- [82] Y. Yu, Z. Li, Y. Wang, S. Gong, and X. Wang, “Sequential infiltration synthesis of doped polymer films with tunable electrical properties for efficient triboelectric nanogenerator development,” *Advanced Materials*, vol. 27, no. 33, pp. 4938–4944, 2015.
- [83] J. Chung, S. Lee, H. Yong, H. Moon, D. Choi, and S. Lee, “Self-packaging elastic bellows-type triboelectric nanogenerator,” *Nano Energy*, vol. 20, pp. 84–93, 2016.
- [84] B. K. Yun, J. W. Kim, H. S. Kim, K. W. Jung, Y. Yi, M.-S. Jeong, J.-H. Ko, and J. H. Jung, “Base-treated polydimethylsiloxane surfaces as enhanced triboelectric nanogenerators,” *Nano Energy*, vol. 15, pp. 523–529, 2015.
- [85] J. Chun, J. W. Kim, W.-s. Jung, C.-Y. Kang, S.-W. Kim, Z. L. Wang, and J. M. Baik, “Mesoporous pores impregnated with au nanoparticles as effective dielectrics for enhancing triboelectric nanogenerator performance in harsh environments,” *Energy & Environmental Science*, vol. 8, no. 10, pp. 3006–3012, 2015.
- [86] T. T. Grove, M. F. Masters, and R. E. Miers, “Determining dielectric constants using a parallel plate capacitor,” *American Journal of Physics*, vol. 73, no. 1, pp. 52–56, 2005.

- [87] E. Hourdakis, B. J. Simonds, and N. M. Zimmerman, “Submicron gap capacitor for measurement of breakdown voltage in air,” *Review of scientific instruments*, vol. 77, no. 3, pp. 34702–34702, 2006.
- [88] M. Hogue, C. Buhler, C. Calle, T. Matsuyama, W. Luo, and E. Groop, “Insulator–insulator contact charging and its relationship to atmospheric pressure,” *Journal of electrostatics*, vol. 61, no. 3, pp. 259–268, 2004.

Appendix A

Arduino codes

Example code for 1 Hz (ON state = 5000 ms and OFF state = 5000 ms):

```
int Button = 8;
int Relay = 2;
int RelayCondition = HIGH;
int ButtonCondition = 0 ;

int ON_State_time = 5000;      // Time is in milli seconds

int OFF_State_time= 5000;     // Time is in milli seconds

int previous = LOW;
void setup (){
  pinMode (Button, INPUT);
  pinMode (Relay, OUTPUT);
}
void loop (){
  ButtonCondition = digitalRead (Button);
  if (ButtonCondition == HIGH && previous == LOW){

  digitalWrite (Relay, LOW);
  delay (ON_State_time);
```

```
digitalWrite (Relay, HIGH);  
delay (OFF_State_time);  
  
if (ButtonCondition == HIGH) {  
  RelayCondition = HIGH ;  
  
  }  
  }  
previous == ButtonCondition ;  
digitalWrite (Relay, RelayCondition );  
}
```

Appendix B

Device control system

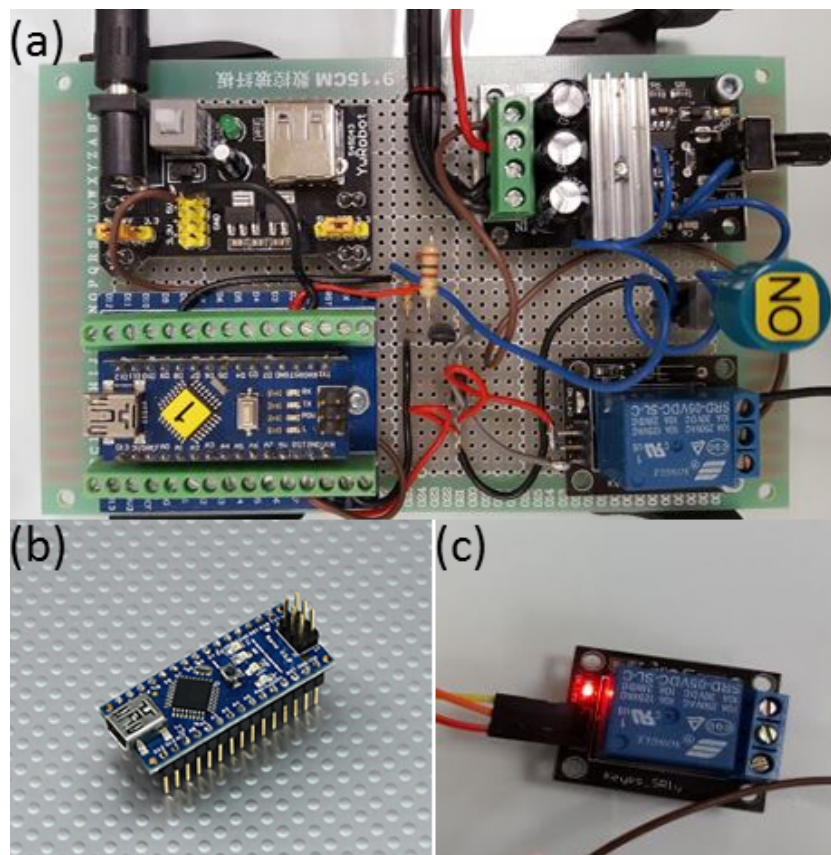


Figure B.1: Electronic components used. (a) Control system of the tapping device used. (b) Microcontroller used in the control system (Arduino Nano), and (c) relay (SRD 0-5VDC-SL-C) used in the circuit.

Appendix C

Circuit diagram

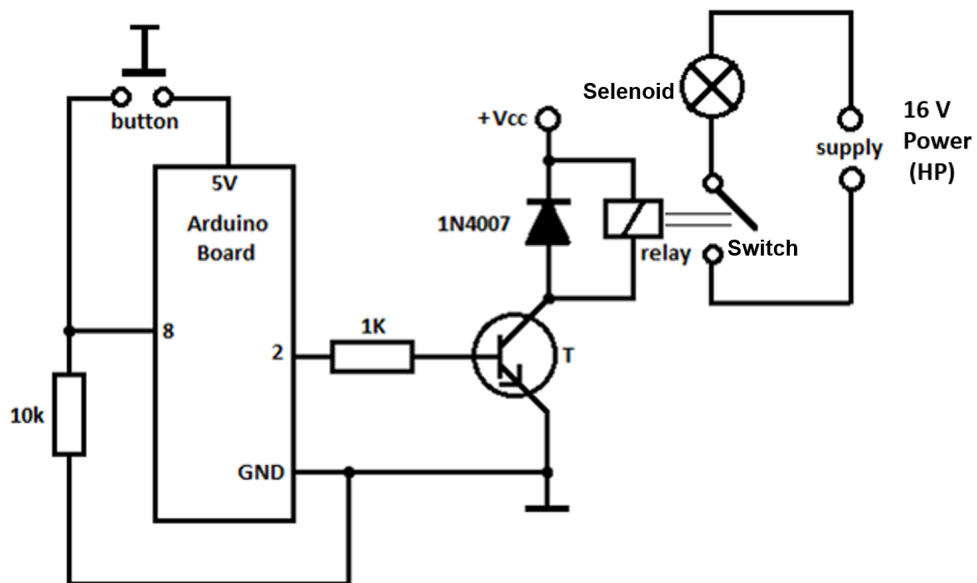


Figure C.1: Electronic circuit used for constructing the ON-OFF switching system of our tapping device.

Appendix D

Data processing

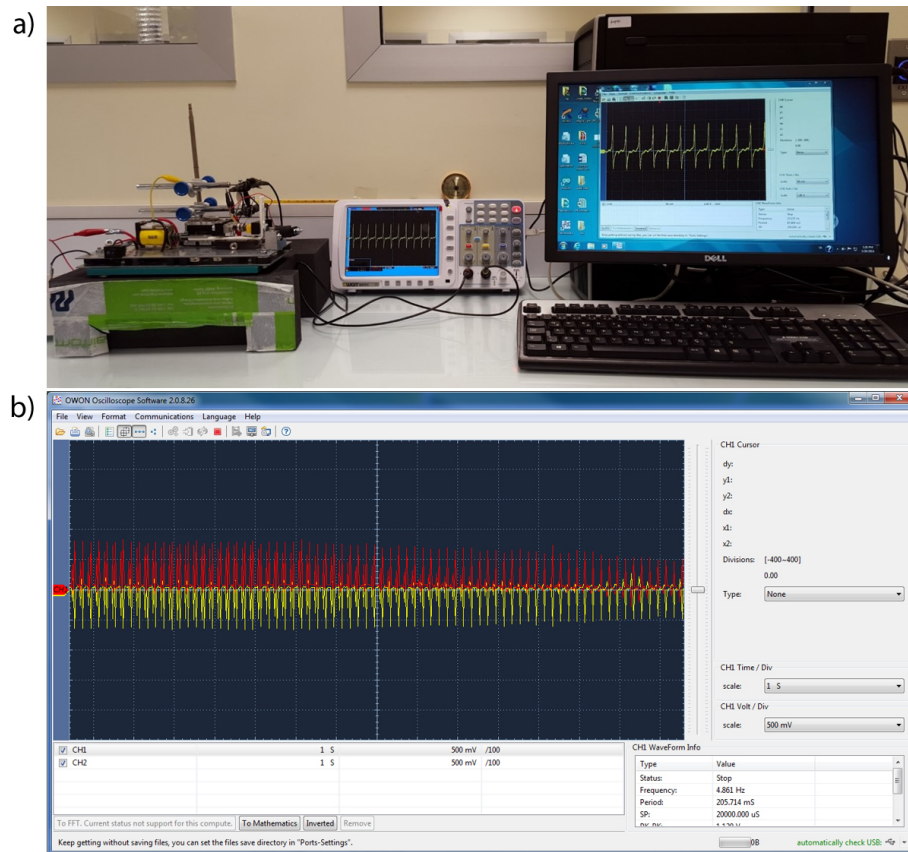


Figure D.1: Signal data processing. (a) Data transfer from OWON oscilloscope to its software. (b) Screen shot of OWON oscilloscope software (version 2.0.8.26).